(4)

FINAL REPORT

prepared for

NAVAL RESEARCH LABORATORY

by

General Coherent Technology, Inc.
1216 Glen Cove
Richardson, TX 75080

describing research accomplishments on

GAMMA RAY LASER PUMP DIAGNOSTIC

supported by
SBIR Contract No. N00014-88-C-2257

Prepared by: C. B. Collins

C B Collins

Principal Investigator

Date: 1/18/89

TABLE OF CONTENTS

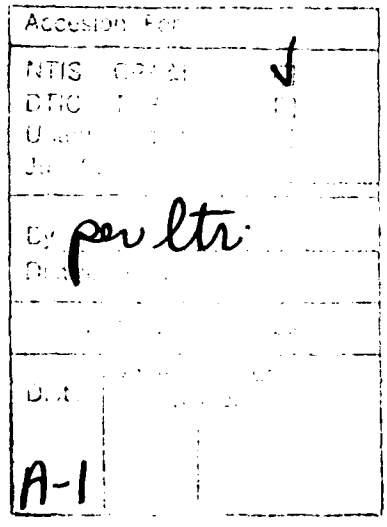

I. Identification and Significance of the Problem

The nuclear analog of the ruby laser would embody the most straightforward of the several concepts[1] for a gamma ray laser. Not surprisingly, the greatest progress toward an ultrashort wavelength laser has been achieved along that direction[2].

For ruby the identification and exploitation of a bandwidth funnel were the critical keys in the development of the first laser. There was a broad absorption band linked through efficient cascading to the narrow laser level. The search for the analogous situation on the nuclear scale is proceeding quite fruitfully. Significant amounts of nuclear fluorescence have been pumped by pulsed bremsstrahlung sources; thus proving that the concept of bandwidth funneling works as well at the nuclear level as it does for the ruby[3]. This critical process was found to produce eleven orders of magnitude increase in the amount of x-ray pump energy absorbed into demonstration nuclei of ^{77}Se.

Most recently, the first of the 29 candidate materials for a gamma ray laser was successfully pumped with intense pulses of bremsstrahlung. The yield of nuclear fluorescence was about 10,000 times greater than what was predicted by even the theories including the large factor for funneling[4]. Selected over 28 alternatives solely on the basis of availability, this first material narrowly missed the threshold of feasibility for a gamma ray laser. These results with a relatively unattractive candidate indicate that the probabilities should be raised for full success of one of the other 28 materials.

While the rate of progress is very high in the existing SDIO Gamma Ray Laser Program, pacing constraints arise from:

1) limitations of supporting technology, and

2) extreme scarcity of the 29 candidate materials. Successes in alleviating the first problem would make it possible to proceed more rapidly without having to overcome the much more expensive aspects of the second problem. Once more advanced technology is available to identify the best of the 29 from minute samples, the problems of the production of useful amounts need only be solved for the one material selected. It was the purpose of this SBIR effort to explore the development of one innovation which can materially advance the technology supporting the Gamma Ray Laser Program.

A number of fundamental factors conspire to make it extremely difficult to accurately measure the spectral content of intense pulses of bremsstrahlung containing photon energies above 200 keV. However this is just the type of pump radiation currently used in testing materials which might serve as nuclear analogs of the ruby system. With no quantitative measures of spectral input, determinations of fluorescence efficiencies are extremely difficult and even the relative rankings of the merits of specific nuclei must be equivocal.

There are no periodic spacings of atoms or lattices comparable to a wavelength at such energies so dispersion is ineffective. In pulsed sources the great number of individual photons insures pile-up in solid state detectors effectively eliminating spectral information. The attenuation of radiation in matter is no longer structured at such energies, so neither selective filtering nor even bandpass layers can be effectively configured. Difficulties are so severe that bremsstrahlung sources of intense pulses are routinely "calibrated" by calculating what the intensity should be. Until this year, this had been the only available procedure for both medical linacs[5] and nuclear simulators[6].

A very recent spinoff of the SDIO Gamma Ray Laser Program at the University of Texas at Dallas has been the technique of X-ray Activation of Nuclei[7,8] (XAN) for the calibration of intense bremsstrahlung sources operating in the range 0.2 to 1.4 MeV. As currently implemented, five isotopes, ^{77}Se, ^{79}Br, ^{111}Cd, ^{115}In, and ^{167}Er are used to sample narrow spectral slices of the bremsstrahlung fluence illuminating a target. The isotopes are excited to long lived states whose nuclear fluorescences can be "read-out" at a later time at which there is less electrical noise. With five isotopes the XAN method accommodates measurement at five photon energies in the range 0.2 to 1.4 MeV.

One of the unexpected results of the pumping of the first actual laser candidate was the importance[9] of nuclear states lying above 1.4 MeV. Unfortunately, these levels could only be accessed by the uncalibrated parts of the source spectrum for which XAN cannot be used. The technical need that was addressed by the research of this Phase I effort was the absolute calibration of the rest[10] of the range of photon energies, 1.4 to 6.0 MeV, which may be useful in studying the candidates. In principle this can be done with an extension of the XAN instrumentation, but the initial calibration and validation will require technology not presently available to the existing gamma ray laser projects nor currently budgeted for development. The research we have completed under Phase I of the SBIR program has proven that the integration and use of the requisite technology is definitely feasible.

II. Technical Background

Energetics of the XAN procedures are shown in Fig. 1. As seen there, the resonant absorption of a bremsstrahlung photon,

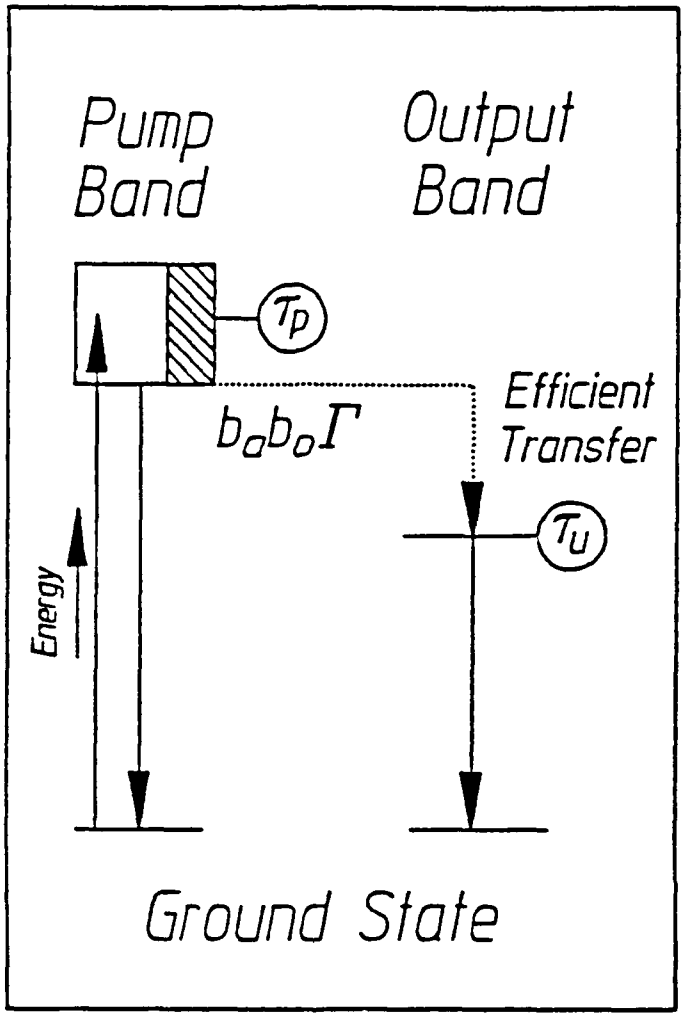

Figure 1: Schematic representation of the energetics of the XAN process for sampling x-ray spectral intensities. Absorption of an x-ray first excites a short-lived state which then decays in part by cascading to a long-lived state.

symbolized by the upward arrow, raises a nucleus from the ground state to a funneling level represented by the partly shaded rectangle. Its extremely short lifetime gives it a relatively broad width for the absorption of a photon from the pump continuum. However, broad at the nuclear level is still narrow in comparison to any structure in the x-rays from the pump, so the

excitation of the funneling level occurs to an extent dependent upon the intensity in a narrow slice of the spectrum of the input radiation. Nonresonant contributions to such excitations have been shown to be negligible[11,12] so the population of the funneling level will be simply proportional to the input intensity at the corresponding energy.

As shown in Fig. 1 by the shaded portion of the rectangle, a fraction b_0 of the population cascades to the longer-lived isomeric state which ultimately radiates the output fluorescence. The complementary fraction b_a decays back to the ground state. The quantitative yield of fluorescence can be written in terms of the spectral fluence input and the nuclear parameters of Fig. 1 in a particularly convenient form here reproduced from Ref. 13 with permission of the authors.

As described in the article reporting the previous implementation of this technique at lower energies, the number of excited nuclei produced in the course of an irradiation of the type shown in Fig. 1 can be computed from the expression:

$$S = N \sum_i \frac{(\pi b_a b_o \sigma_o \Gamma/2)_i}{E_i} \quad \frac{\phi(E_i)}{A} \quad , \qquad (1)$$

where N is the number of absorbing nuclei in the sample and the summation is taken over the properties and pump fluxes characteristic of each of the i-th broad pump bands centered at pump energy E_i. Only one such pump band is shown in the scheme of Fig. 1, but there could be several at different E_i, each funneling its population into the same output level.

In Eq. (1) the first ratio in the summation is composed of the nuclear parameters, while the second describes the intensities of the pump x-rays which are assumed to be continuous, at least without structure on the fine scale of the nuclear absorption. In particular, the combination $\phi(E_i)/A$ is the spectral fluence at the energy E_i in units of keV/keV/cm^2. Tacitly, it has been assumed that the duration of the pump source is less than the fluorescence lifetime, τ_u.

Of the nuclear parameters, Γ is the natural width in keV of the i-th pump band, as shown in Fig. 1,

$$\Gamma = \hbar/\tau_p \quad , \tag{2}$$

and the branching ratios, b_a and b_o, give the probabilities for the decay of the broad level back into the initial and fluorescence level, respectively. The pump energy, E_i, is in keV and σ_o is the Breit-Wigner cross section for the absorption transition,

$$\sigma_o = \frac{\lambda^2}{2\pi} \quad \frac{2I_e+1}{2I_g+1} \quad \frac{1}{\alpha_p+1} \quad , \tag{3a}$$

where λ is the wavelength in cm of the gamma ray at the resonant energy, E_i; I_e and I_g are the nuclear spins of the excited and ground states, respectively; and α_p is the total internal conversion coefficient for the broad level of Fig. 1.

The combination appearing in parentheses in the numerator of the "nuclear part" of Eq. (1) is the integrated cross section which is conveniently measured in units of 10^{-29} cm^2 kev,

$$q_i = (\pi b_a b_o \sigma_o \Gamma/2)_i \quad . \tag{3b}$$

This expression is most often used in numerical computation, followed closely by,

$$Q_i = q_i/E_i \quad , \tag{3c}$$

and the effective partial width for excitation of the output channel,

$$G_i = (b_a b_o \Gamma)_i \quad . \tag{3d}$$

On this scale for integrated cross sections, q_i unity or even a few tenths suffice for a material to be useful in

sampling spectral fluences of the order of 10^{12} to 10^{14} keV/keV/cm^2 at the corresponding energy. These integrated cross sections are the critical numbers which must be determined before XAN can be used for calibrating bremsstrahlung sources. For example, the entire database[2] which currently supports use of the XAN process for calibrating nuclear simulators over the 0.2 to 1.4 MeV range of energies is shown in Table I. It is the extension of this tabulation to a higher range of energies that comprised the larger objective of this work. How to accomplish this goal was the particular subject of this effort.

It has already been established[14] that even the most current nuclear database[15] of general use does not offer significant precision for nuclear parameters such as b_a b_0 to allow the cross sections to be calculated to a useful accuracy. To determine them currently requires the application of Eq. (1) to sets of fluorescence data actually measured. It can be readily appreciated that sequences of measurements of the numbers of isomeric nuclei, S_m produced in the m-th particular irradiation delivering fluences of $F_m(E_i)$ at each of the energies E_i corresponding to a gateway cascading to the isomer lead to a set of equations,

$$S_1 = Q_1F_1(E_1) + Q_2F_1(E_2) + \ldots \quad , \quad (4a)$$
$$S_2 = Q_1F_2(E_1) + Q_2F_2(E_2) \quad , \quad (4b)$$
$$S_3 = Q_1F_3(E_1) \quad , \quad (4c)$$

where the Q_i are the combinations of nuclear parameters comprising the first ratio in Eq. (1) for the gateway at E_i. In principle, the technique for determining the set of Q_i consists of measuring the S_m obtained with a number of different spectral distributions $F_m(E_i)$ and then solving the set of equations for the Q_i. In practice, the problem is much more difficult. The gateway energies, E_i are not usually known, and the problem of

Table I

Summary of nuclear parameters for applications of the X-ray Activation of Nuclei at energies below 1.4 MeV.

Nuclide	E_{in} (keV)	E_{out} (keV)	Integrated Cross Section (10^{-29} cm^2 keV)
^{79}Br	761	207	6.2
^{77}Se	250	162	0.20
	480[a]		0.87
	818		0.7
	1005		30.0
^{115}In	1078	337	20.0
^{111}Cd	1190	245	9.8
^{167}Er	900	208	23.0

[a]The effects of the 440 and 521 keV transitions have been combined.

determining the $F_m(E_i)$ is the general one motivating the measurements of the Q_i.

The key to the solution of the problem lies in Eq. (4c). By adjusting the end point energy of the irradiation to successively lower values, the $F_m(E_i)$ can be made zero for all but the lowest energy gateway, E_1. Then, there is only one term on the right. Further adjustment of the end point will identify that gateway energy by turning off the yield, as seen in the example shown in Fig. 2. There, E_1 is clearly indicated by the intercept.

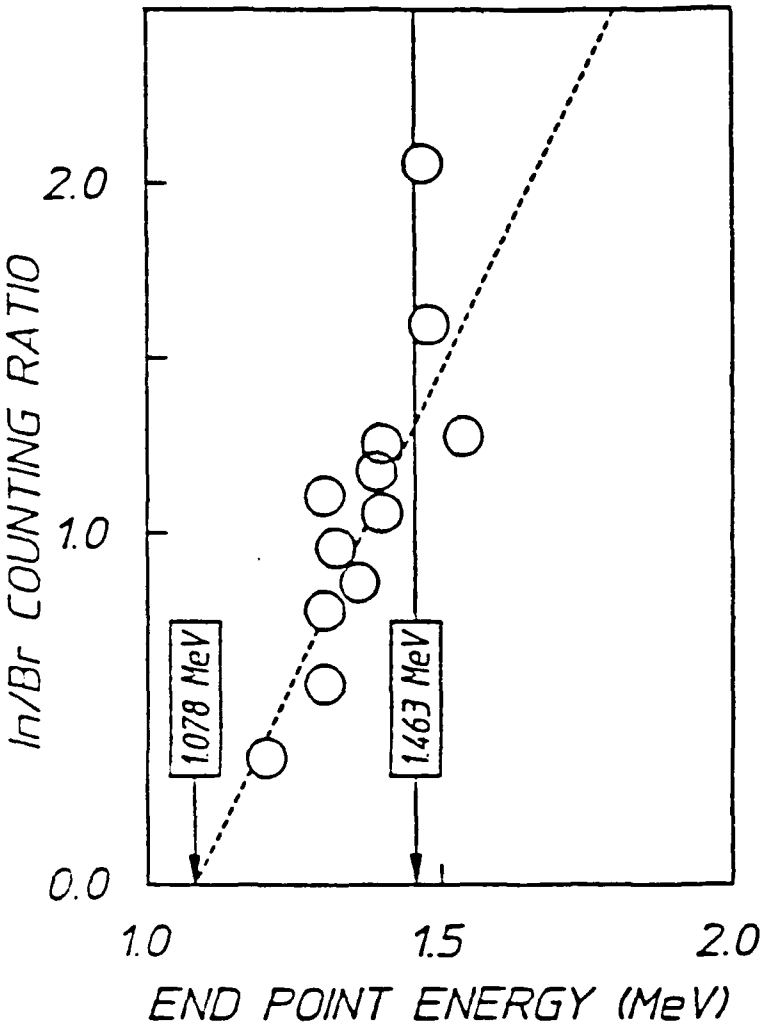

Figure 2: Nuclear fluorescence from ^{115m}In normalized to ^{79m}Br pumped by single pulses of bremsstrahlung having end point energies shown. The linear fit to the data intercepts the axis at a gateway energy of 1.078 MeV.

Once the lowest gateway energy is determined, Eq. (4c) can be solved for the first cross section,

$$Q_1 = S_m / F_m(E_1) \quad , \quad (5)$$

where the free index, m implies that Q_1 can be determined as

an average from a number of measurements. It is not rigorously true that spectral content can never be measured for any bremsstrahlung. If intense pulsed sources can be fired with reasonable cost and repetition rate, they can be observed with a geometry insuring that only one photon reaches a detector per pulse. In that case the energy of that photon can be determined and logged before the next pulse and in this way the spectrum of the bremsstrahlung can be collected as an experimental probability of detecting a photon of a given energy. From the geometry the total number of photons can be determined at a particular energy for a given duration of the m-th exposure producing the measured number of activations, S_m. Then, of course, Eq. (5) can be used to extract a value of Q_1 which can subsequently be used to determine fluences at E_1 from any other sources by measuring only the S they produce.

Once the first Q_1 is found, Eq. (4b) can be used to determine the next with measurements made with a higher end point energy,

$$Q_2 = (S_m - Q_1 F_m(E_1)) \; / \; F_m(E_2) \; . \quad (6)$$

In actual practice a great amount of care is necessary to insure that changes of end point energy do not open more than one gateway at a time and to collect sufficient statistics for the $F_m(E_i)$ so that the differences implied by Eq. (6) do not degrade the determinations of the Q_i.

It appears that only variable energy linacs have the combinations of parameters needed to meet these requirements and one must be procured in subsequent stages of this development. Once the equivalent of Table I is produced in this way for the range of energies from 1.4 to 6.0 MeV, the continuum from any source can be measured directly with a simple set of foils and a

counting system.

III Phase I Accomplishments

Our Phase I modeling has shown that gateway energies for the activation of 19 stable isotopes could be measured with a variable energy linac which will be needed for the next phase of this research. The scaling of preliminary measurements with a fixed energy linac has proven that sensitivities of all 19 materials are sufficient for use in sampling the spectral content of a single shot from a nuclear simulator of the scale of DNA/AURORA, as well as the spectrum from a linac of the type used for medical radiation therapy during the few minutes period each day set aside for calibration. The viability of a commercial instrument or service seems very clear, once the nuclear properties of the 19 are standardized in subsequent work.

The principal risk is that all isotopes might conceivably sample the same slice of the spectrum and so be unable to record spectral intensities at energies other than at that single value. Were there only two or three usable isotopes, such a possibility might be cause for concern. However, the chances that 19 isotopes would have indistinguishable absorption spectra is too remote for serious consideration. Such concern is more properly reduced to the status of a problem; a problem in optimizing the best spectral coverage with the most economical target package. That is part of the work needed in a future effort.

The details of the accomplishments of Phase I upon which rest the strongly positive assessment of feasibility are reviewed below.

III.1 The 19 sampling isotopes.

Appearing in Table II is a proprietary listing of the 19 stable isotopes known to activate when irradiated by the fluence accumulated from a 6 MeV Varian CLINAC 1800 in a few minutes. Shown there is the isomer and its abundance in naturally occurring material in the first two columns. In the next columns are the energies of the isomeric levels and their lifetimes for storing the samples of the irradiating spectrum to which they are sensitive. Then follow statistical quantities for use in Eq. (3a) with the identification. $I_e = J_i$ and $I_g = J_g$. Finally, in the last column of Table II is the most important quantity, the integrated cross section, q of Eq. (3b).

Since the energy, E_i of the gateway for the activation of a particular isomer is not known, the individual cross sections cannot be expressed as the q_i for a given E_i. That is the problem onto which the next phase of work must be focused. Rather, in Table II the artifice has been employed of computing the value of q which would have been required to produce the observed activation through a gateway of 2.125 MeV which is most probably the lowest value at which such a large activation could occur.

The cross sections of Table II were determined from the absolute activations resulting from irradiations with the spectrum shown in Table III. As can be seen, it has been normalized to unit spectral intensity at 2.125 MeV. Had the gateway, E_i in a particular case opened at a higher energy, then the observed amount of product would have resulted from a spectral intensity lower than assumed and the actual value of cross section would be larger than what is shown in Table II by

Table II

Summary of the properties of isomers known to activate through giant gateways opening in the range of energies between 2 MeV and 6 MeV. Values for q, the integrated cross section of Eq. (3b) are taken from Ref.16. Since the gateways are unknown, the cross sections have been reported as values pertaining to a standard, arbitrary reference energy of 2.125 MeV.

Isomer	Ground State Abundance (%)	Energy (MeV)	Isomeric Halflife		J_g	J_i	q (10^{-29} cm^{2}keV)
$^{77}Se^m$	7.6	0.162	17.45	s	1/2-	7/2+	7810
$^{79}Br^m$	50.69	0.207	4.864	s	3/2-	9/2+	2180
$^{87}Sr^m$	7.0	0.388	2.81	h	9/2+	1/2-	1004 ± 6
$^{89}Y^m$	100.0	0.909	16.06	s	1/2-	9/2+	296
$^{111}Cd^m$	12.8	0.396	48.6	m	1/2+	11/2-	3300 ± 480
$^{113}In^m$	4.3	0.392	1.658	h	9/2+	1/2-	5000 ± 260
$^{115}In^m$	95.7	0.336	4.486	h	9/2+	1/2-	6700 ± 620
$^{117}Sn^m$	7.68	0.315	13.61	d	1/2+	11/2-	1050 ± 70
$^{123}Te^m$	0.91	0.247	119.7	d	1/2+	11/2-	8100 ± 200
$^{135}Ba^m$	6.59	0.268	28.7	h	3/2+	11/2-	6520 ± 110
$^{137}Ba^m$	11.74	0.662	2.5513	m	3/2+	11/2-	2120
$^{167}Er^m$	22.95	0.208	2.28	s	7/2+	1/2-	43200
$^{179}Hf^m$	13.63	0.375	18.68	s	9/2+	1/2-	31000 ± 500
$^{180}Ta^m$	0.00	0.032	1.2×10^{15}	y	1+	9-	49000
$^{183}W^m$	14.3	0.309	5.15	s	1/2-	11/2+	2220
$^{191}Ir^m$	37.3	0.171	4.94	s	3/2+	11/2-	41400
$^{195}Pt^m$	33.8	0.259	4.02	d	1/2-	13/2+	20900 ± 1200
$^{197}Au^m$	100.0	0.409	7.8	s	3/2+	11/2-	15300 ± 1100
$^{199}Hg^m$	16.84	0.532	42.6	m	1/2-	13/2+	1849 ± 45

Table III

Ratios of the photon intensities at energies E to that at 2.125 MeV for the spectrum used in the measurements of Table II.

Energy (MeV)	$r=\Phi(E)/\Phi(2.125)$
0.125	0.015
0.375	0.500
0.625	1.731
0.875	1.769
1.125	1.654
1.375	1.538
1.625	1.538
1.875	0.962
2.125	1.000
2.375	0.731
2.625	0.538
2.875	0.500
3.125	0.615
3.375	0.354
3.625	0.500
3.875	0.385
4.125	0.346
4.375	0.204
4.625	0.162
4.875	0.188
5.125	0.065
5.375	0.108
5.625	0.050
5.875	0.065

the compensating amount. For example, if a particular E_i were found to be 2.875 MeV rather than the arbitrary reference value of 2.125 then Table III shows that the actual integrated cross section, q_i should be twice the value of q shown in Table II. Generally, if there is single gateway at E_i, then,

$$q_i = q/r(E_i) \quad . \quad (7)$$

The situation with multiple gateways is more complex and the equivalent expression is found from the relation,

$$q = r(E_1)q_1 + r(E_2)q_2 + ... \quad (8)$$

The decomposition of q into the individual q_i can only be done experimentally, as expected in a future phase of effort. However, nuclear systematics provide guidance sufficient to show the clear feasibility of such experiments. Moreover, they serve to identify seven candidates for the role of primary norm.

III.2 Nuclear Systematics and the Primary Norm

Completed during this Phase I of research has been a study of the systematics of the nuclear properties contributing to the occurrence of giant gateways for activation such as those shown in Table II. Figure 3 shows a plot of the integrated cross section, q as a function of the mass number, A of the nucleus being activated.

Of great importance in Fig. 3 are the two triangular data points which record the only two cases for which the E_i have been determined for excitation of isomers through giant gateways. Those two isotopes[17,18] were ^{87}Sr and ^{197}Au. For consistency, the integrated cross sections in both cases have been "corrected" back to 2.125 MeV for plotting through use of the inverse of

Eq. (7). The data point for ^{197}Au is shown as a part of the total q of Eq. (8) that was separated by an ad hoc procedure[18] applicable only to that material.

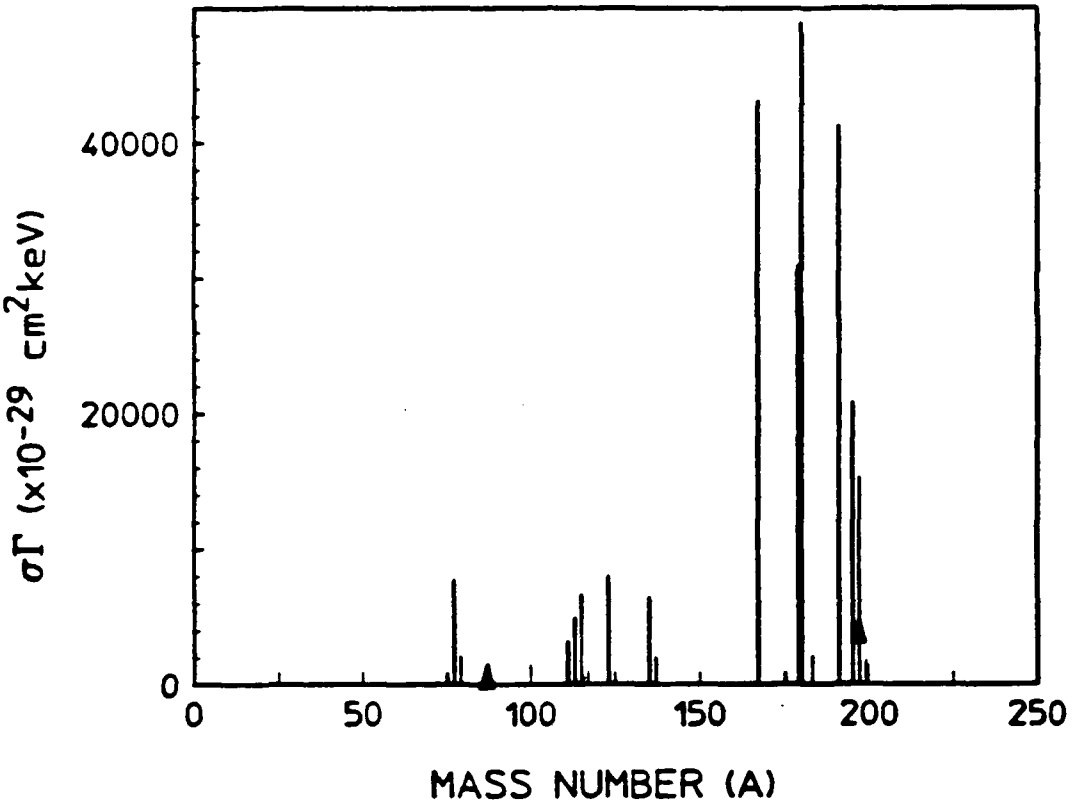

Figure 3: Plot of the integrated cross sections, q as functions of the mass number of the nuclei listed in Table II. Triangles plot data points for individual q_i where values are available from Refs. 17 and 18 for ^{87}Sr and ^{197}Au, respectively.

Even a cursory inspection shows several trends worthy of note. With the exception of the anomalously large value for ^{77}Se, the other 18 isotopes seem to group into three islands, the

peaks of which appear to scale up by about a factor of five from the one immediately preceding. Countering this general trend is a distribution of much smaller values which seem to vary little over the whole span of masses.

Since the funneling process of Fig. 1 should not work so well for purely single particle states of nuclear excitation, it has been hypothesized that collective excitation of several core nucleons could break symmetries, tending to hinder the transitions of Fig. 1 because of selection rules on projections of angular momenta. At the same time, the collective excitation of several particles would tend to enlarge the magnitudes of the matrix elements coupling the nucleus to the radiation field so that transitions would occur with the same multipolarities as indicated by the ΔJ for the transition.

The general scaling of electromagnetic transition rates when single particles mediate the transitions is given by a number of authors[21] in forms equivalent to,

$$W(QUAD) = C_Q A^{4/3} E^5 \quad , \quad (9)$$

for quadrupole transitions, and

$$W(OCT) = C_0 A^2 E^7 \quad , \quad (10)$$

for octupole transitions. While it is extremely speculative to attempt to fit cause to the experimental effects recorded in Table II, there is no theoretical guidance, so perhaps some empiricism is justified. There is nothing else possible until further work is completed.

It has been reported[20] that collective octupole transitions should be much stronger than quadrupoles because the symmetries

of such vibrations tend to release the otherwise hindered electric dipole components of a transition. In that case we might reasonably identify the smaller distribution of cross sections with the less effective collective quadrupole vibrations. Then, using the known values shown in Fig. (3) for the two data points, $r(E_i)q_i$ for ^{87}Sr and ^{197}Au allows for the determination of $C_Q E^5$ in Eq. (9). The resulting fit is shown in Fig. 4 where the dotted curve plots the value,

$$W_Q = 1000(A/87)^{4/3} \quad , \quad (11)$$

in the usual units of 10^{-29} $cm^2 keV$.

A magnification of the relevant portions of Fig. 4 is shown in Fig. 5. The agreement to the expression of Eq. (11) of the data for the seven isomers specifically identified is much better than could be reasonably expected, were there not some merit in the approximations being employed.

As a working hypothesis for further analysis, it was assumed that the seven elements summarized in Table IV were activated through a single gateway lying in the quadrupole region between about 1.5 and 3.0 MeV. The much greater total cross sections of the other isotopes were then attributed to the contribution of a larger gateway opening at higher energies. This was known to be the case for the only system studied in detail previously, ^{197}Au. For use in our computations, the q_i for the seven isotopes most likely to be single gateway materials were obtained from

$$q_i = 1000(A/87)^{4/3}/r(E_i) \quad . \quad (12)$$

The role of such single gateway isotopes as normalizing standards is extremely important in the measurement of spectral intensities, and it is encouraging to reflect that success in

implementing the XAN process over the lower energy range, 0.2-1.5 MeV required only one such selective nuclei, ^{79}Br over that range. Here, for this case there are seven potential standards. Any one of them would be viable as a primary norm. Probabilities are very high that one can be proven experimentally while the others are used to provide convenient spectral detail.

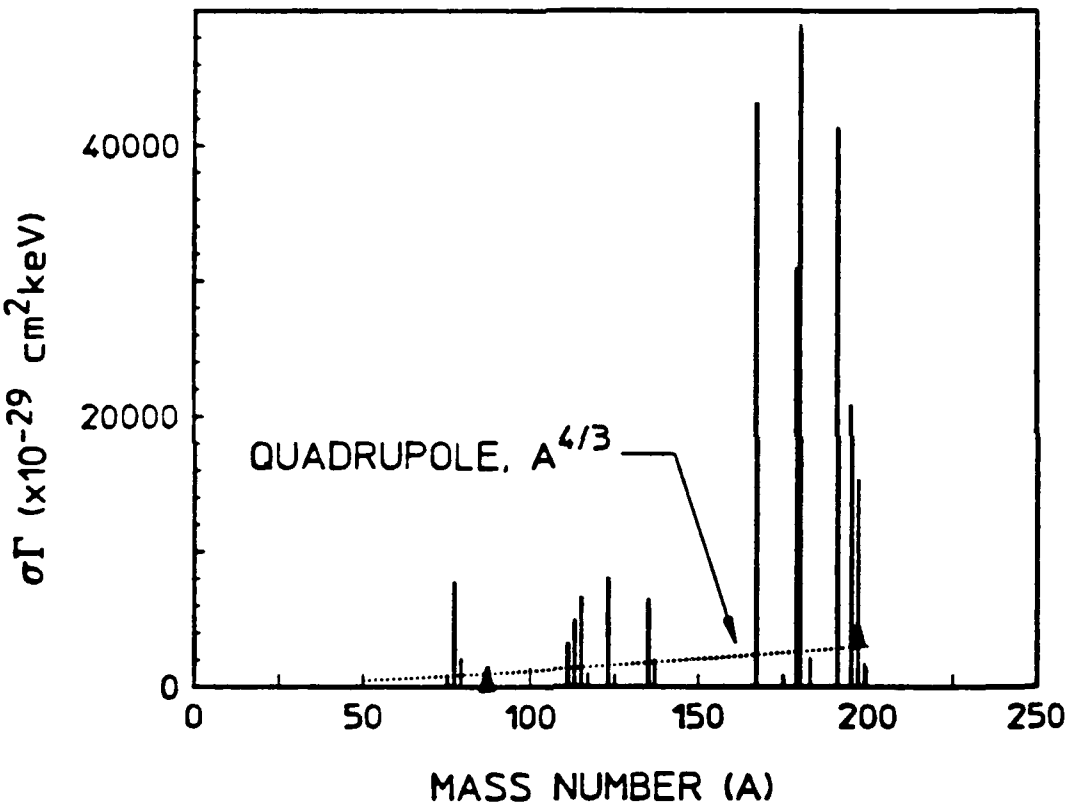

Figure 4: Plot of the integrated cross sections, q as functions of the mass number of the nuclei listed in Table II. The dotted curve shows the scaling of transitions mediated by a giant quadrupole oscillation.

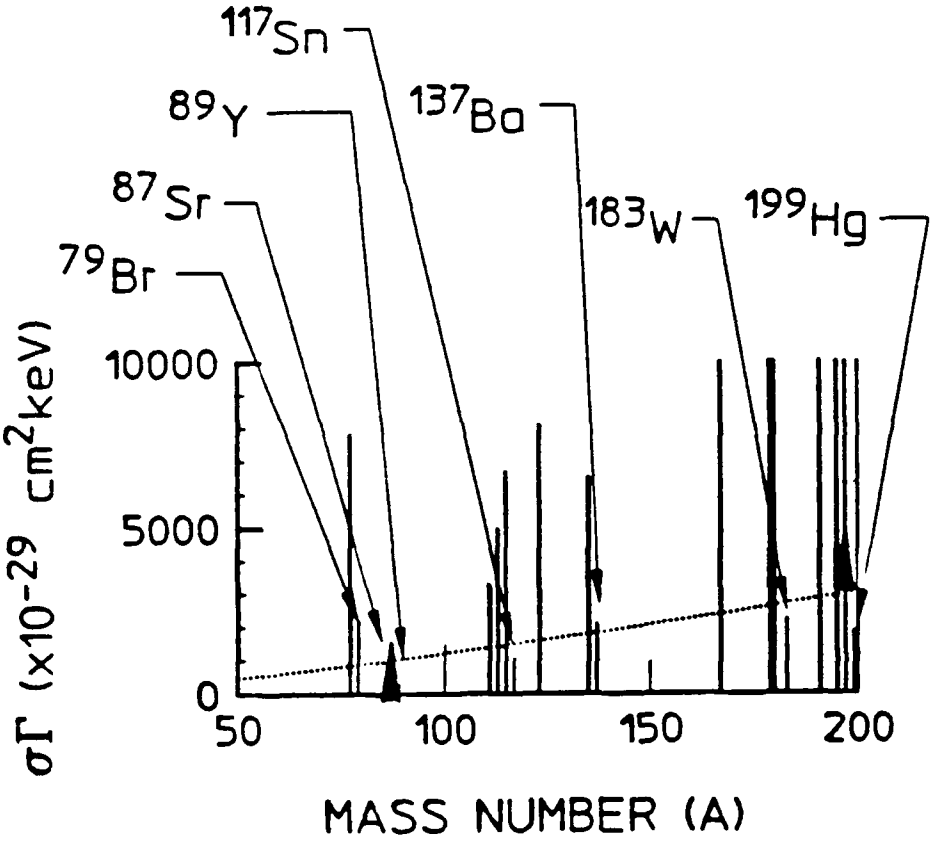

Figure 5: Magnification of a portion of Fig. 4 plotting values of the integrated cross sections, q from Table II as functions of mass number. Isotopes are identified whose cross sections seem to agree with the approximation of Eq. (11) shown by the dotted curve.

Table IV

Isotopes identified in Phase I studies as the most likely to have single gateways for activation in the 2-6 MeV range. These are the trial standards for subsequent validation. Recorded in the rightmost column are the integrated cross sections, q obtained from the smoothing approximation for quadrupole transitions, Eq. (12) normalized to 2.125 MeV for convenience by Eq. (7).

Isotope	Abundance (%)	Storage Halflife	q(2.125) (10^{-29} cm^2 keV)
^{79}Br	50.69	4.86 s	880
^{87}Sr	7.0	2.81 h	1000
^{89}Y	100	16.06 s	1030
^{117}Sn	7.68	13.6 d	1480
^{137}Ba	11.74	2.55 m	1830
^{183}W	14.3	5.15 s	2690
^{199}Hg	16.84	42.6 m	3010

III.3 Measurement Strategies

Even an *a priori* choice of a primary norm from the group of seven candidates would be dominated by what is now a free choice of the functional cycle. There are two classes of operation to consider. The most versatile is a "pop-in" strategy which is also the most expensive to engineer as a subsequent product or service. There the transfer from the point of irradiation to the place of measurement is done pneumatically or mechanically. With such a system the time lost in transfer can be as little as a second so that even the isotopes with the shortest storage times can retain enough activation for accurate read-out. However, the complexity of such a system is so much greater than for the alternative, any strategy for commercialization would require first preference be given to the other technique. Because of this, the principal emphasis in Phase I was placed on the alternative cycle with the intention to switch to the "pop-in" approach if it became clear that either accuracy or resolution was being unduly compromised. That necessity has not yet been perceived.

The preferred strategy for the implementation of XAN is a passive one in which a target package is placed in the area to be irradiated by an operator or technician. Allowing operator choice permits the precise point of medical treatment or simulated blast impact to be instrumented with the ultimate flexibility. After irradiation the operator returns to detach the target and insert it into a counting chamber which is properly shielded to insure a low background. An answer would be desirable within a time comparable to that for irradiation, transport and handling, and that implies only a part of the activation will be counted during that arbitrary standard

interval. Each step of treatment is associated with a loss of activation, and hence, a reduced sensitivity that will change the figures of merit associated with each of the candidate norms of Table IV from being simply dependent upon the value of q(2.125).

For the modeling of the efficiencies for the use of any of the candidate norms, it is necessary to obtain an effective value of integrated cross section, q' that has been corrected for the varying amounts of loss of activation imposed by the particular operating cycle planned,

$$q'_{eff} = abcq \quad , \quad (13)$$

where b is the loss of activation during transfer,

$$b = \exp(-wt_t) \quad , \quad (14a)$$

where c is the fraction of the activation which fluoresces during the counting period,

$$c = 1-\exp(-wt_c) \quad , \quad (14b)$$

where w is the storage lifetime of the activation and t_t and t_c are the times for transfer and counting, respectively. The correction factor, a for the decay of the activation during the finite duration, t_r of the irradiation is unity for the case of impulsive excitation, but otherwise is

$$a = (wt_r)^{-1}(1-\exp(-wt_r)) \quad , \quad (14b)$$

where a has been written to correct activation per unit dose (as opposed to dose rate).

Choosing the modeling parameters for validating medical

therapy machines,

$$\text{irradiation time, } t_r = 10 \text{ min.} \qquad (15a)$$
$$\text{transfer time, } t_t = 2 \text{ min.} \qquad (15b)$$
$$\text{counting time, } t_c = 10 \text{ min.,} \qquad (15c)$$

values which create little operator stress, the resulting figures of merit for the candidate norms can be computed from Eq. (13). However, another important aspect warrants inclusion in this type of effective cross section and that is the fractional abundance, f of the isotope so that

$$q_{eff} = fq'_{eff} = abcfq \quad . \qquad (16)$$

This quantity more nearly approximates the useful activation per input dose per unit amount of target material. It is tabulated in Table V for the seven candidate norms. The comparative values for impulsive excitation, for which a = 1, are also shown.

III.4 Preferred Norms

It is clear from Table V that two of the seven isotopes are preferred choices for use as primary norms, ^{137}Ba and ^{199}Hg. Even with the rather relaxed, passive strategy for measurement the effective cross sections for activation remain in the 10-100 ($\times 10^{-29}$ cm^{2}keV) region we have characterized as describing giant quadrupole transitions. Both considerably exceed the value of 6.2 which was sufficient for ^{79}Br to serve as a norm in the energy range below 1.5 MeV. However, they differ from each other in the details of usage.

The mercury isotope, ^{199}Hg appears to be the ideal norm. No other isotope of mercury activates and the time for decay of the signal is long enough that several successive read-out cycles

would be possible in the event operator error were suspected. Conversely, it is not so long that the sample could not be reused the next day without the need for making a baseline measurement of residual activation before sampling. If more frequent validation of the source were desired, mercury is inexpensive enough that several samples could be stocked to avoid the nuisance of counting residual activation.

Table V

The effective values of integrated cross sections for the isotopes possibly useful as primary norms which relate signal read-out to applied dose in a passive sampling geometry creating low operator stress.

Isotope	Environment	
	q_{eff}, Medical Therapy ($X10^{-29} cm^2 keV$)	q_{eff}, Simulation ($X10^{-29} cm^2 keV$)
^{79}Br	0.00	0.00
^{87}Sr	2.76	2.81
^{89}Y	0.22	5.80
^{117}Sn	0.04	0.04
^{137}Ba	39.90	116.5
^{183}W	0.00	0.00
^{199}Hg	68.00	73.67

The ^{137}Ba is even more favorable in these regards, and its desirability as a primary norm is lessened only by the activation of the ^{135}Ba component of natural barium present in comparable abundance. This latter constituent has a half life over a day and will gradually accumulate activation which will contribute some noise to the counting environment. However, since the more comprehensive measurement strategies anticipate the use of ^{135}Ba as a multiple gateway material, the recycling of this isotope appears inevitable. As long as the bookkeeping is done to record residual activation, then ^{137}Ba becomes almost as attractive a primary norm as ^{199}Hg.

The conclusion of this part of the Phase I analysis is:

Primary Norm - ^{199}Hg
Secondary Norm - ^{137}Ba.

III.5 Quadrupole and Octupole Transitions

For the 12 isotopes appearing in Table II that do not appear in Table IV, the indication is that their much larger value of integrated cross section is contributed by the opening of a giant octupole resonance at higher energy. There may or may not also be a quadrupole resonance, so that these are most probably multiple gateway materials. That is the case of ^{197}Au, the only isotope for which such gateways have been approximately located.[18]

The relative size of octupole cross sections to the quadrupoles is so great that plots of total q can be compared to parameterizations such as Eq. (10) for octupole transitions with little error, even if the quadrupole contributions are not removed. In Fig. 6 the approximations of Eq. (10) are plotted by solid curves for two cases that might reasonably bound the

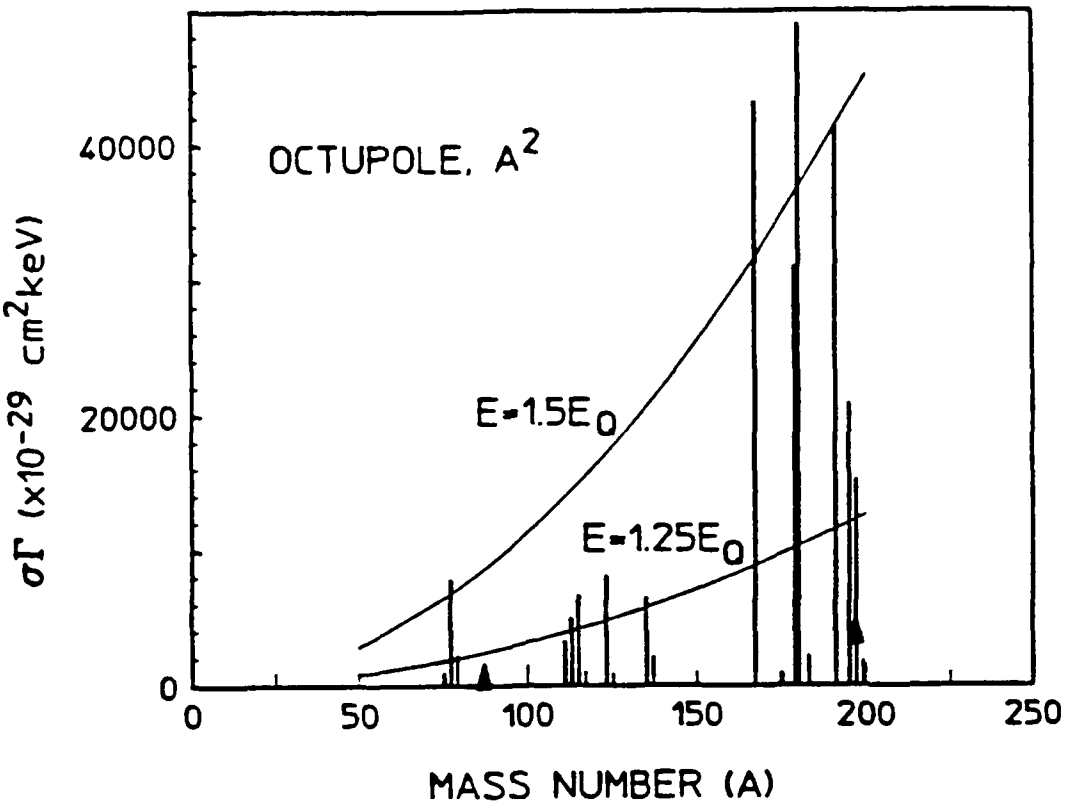

Figure 6: Plot of the integrated cross sections, q as functions of the mass numbers of the nuclei listed in Table II. The solid curve shows the scaling of transitions mediated by giant octupole oscillations. Energies of the octupole gateways are given in terms of the energies of quadrupole transitions for the same isotope.

majority of isotopes. Recalling that data in Fig. 6 are scaled down to 2.125 MeV by Eq. (8), then only the ratio of the E_0 for the octupole resonance to the E_Q for the quadrupole resonance need be raised to the seventh power in Eq. (10) so that

$$W_O = 500(A/87)^2(E_O/E_Q)^7, \qquad (17)$$

where the value of C_O has been chosen to be 500 to fit the data near A = 200. As seen in the figure, the octupole gateways would seem to lie between 1.25 E_Q and 1.5 E_Q. Again, the level of agreement is surprising just as in the case of fitting the single quadrupole gateways in Fig. 5. However, in this case, the exponent of the dependence on energy is so great that actual values are to be preferred over those given by Eq. (17).

III.6 Measurement Modeling

An important concern is whether there are enough of the isotopes with octupole transitions and storage lifetimes long enough to be compatible with the passive measurement strategy mentioned above. Table VI summarizes the effective cross sections from Eq. (16) for those isotopes of Table II having octupole transitions not reduced to zero by the losses in transfer, and by the brevity of the counting interval.

Recalling that Table I shows cross sections as small as 0.2 to have been useful in measuring spectral intensities at energies below 1.5 MeV, it can be seen from Table VI that there are seven usable octupole transitions, even for the most convenient strategy of measurement. The full cross sections of 10,000's of units would be available in a "pop-in" system, but as yet, analysis does not mandate the extra difficulties. It seems preferable to exploit the large size of the octupole transitions to create enough activation that some can be wasted by the simpler procedures for handling the samples that would be most useful in a practical device.

Since each of the materials of Table VI is presumed to have at lease two energies E_i at which spectral intensities are sampled, there are 14 points from the isotopes of that list and

another four from Table V. In all, there are expected to be 18 points at which the intensities are recorded.

Table VI

The effective values of integrated cross sections for the isotopes apparently having octupole transitions. These quantities relate signal read-out to applied dose in a passive sampling geometry creating low operator stress.

Isotope	Environment	
	q_{eff}, Medical Therapy ($X10^{-29} cm^2 keV$)	q_{eff}, Simulation ($X10^{-29} cm^2 keV$)
^{77}Se	0.21	5.00
^{111}Cd	50.9	54.6
^{113}In	14.8	14.8
^{115}In	164	164
^{135}Ba	1.7	1.7
^{179}Hf	2.2	49.2
^{195}Pt	8.5	8.5

If we imagine the sampling points arranged in an ascending series of activation energies, they will comprise a set of energies, E_i where i runs from 1 to 18. They will be distributed over a range from 2 MeV to some maximum assumed to be 6 MeV. The differences

$$X_i = E_i - E_{(i-1)} \quad , \quad (18)$$

where E_0 = 2 MeV, then comprise a set of random variables whose sum is conserved at 4 MeV. The average is X = 0.222 MeV. These intervals X_i and sampling points follow the same statistics as particles in an ideal gas and their kinetic energies. It can be shown that the relative probability of a particular X_i is

$$P_i = \exp(-X_i/X) \quad , \quad (19)$$

and the normalized probability, P_i should be,

$$dP_i = \exp(-X_i/X)d(X_i/X) \quad . \quad (20)$$

The integration of Eq. (20), then shows there to be a proability of only 11% that there will be a gap larger than 0.5 MeV that is not sampled by one of the 18 transitions of the isotopes listed in Tables V and VI.

This seems a reasonable likelihood of an adequate resolution for the measuring process being modeled.

The actual computational procedure to be followed for unfolding the spectrum from the set of activations it produces in the 11 isotopes used for sampling will depend upon the particular energies sampled by the single gateway materials. Depending upon their arrangement in the interval of energies from 2 to 6 MeV, the unfolding process will be either interpolative or

extrapolative, or more likely, a combination of these techniques. The following example is illustrative.

The spectrum of no source is well enough known to be used without further arbitrary assumptions. However, at least the distribution of energies sampled is well known from Table I over the range from 0.2 to 1.5 MeV, so this range is the one preferable for an example. For these energies the linac spectrum of Table II can be simply scaled along the abscissa to fit an endpoint of 1.5 MeV, as shown in Fig. 7.

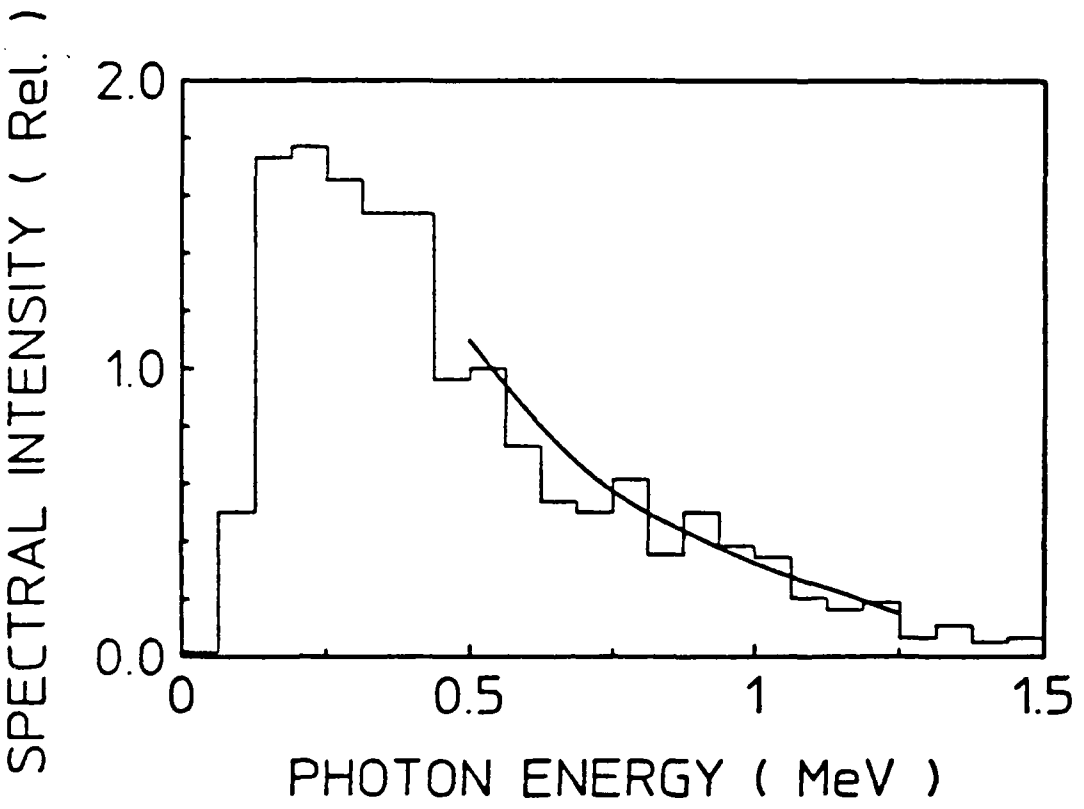

Figure 7: Plot of a hypothetical linac spectrum obtained by scaling the data of Table II to the energy interval shown. The solid curve shows the arbitrary fit of a smooth curve to this data.

To avoid introducing a favorable bias which might occur through use of a power series, an arbitrary curve was fit by hand to the data of Fig. 7 as shown by the solid curve. Had a power series been used, then the same order of series would have allowed the subsequent unfolding to be exact, and so minimized the intrinsic difficulties of the problem. In contrast, a fit by hand gives an unknown mathematical form.

Neglecting the minor contribution of the gateway at 250 keV in ^{77}Se, the matrix for the computation of Eq. (1) can be written as shown in Table VII. The activation of a particular isotope, ^{77}Se for example, can be seen to be

$$S_1 = Q_1F(E_1)+Q_3F(E_3)+Q_4F(E_4) \quad (21a)$$

while the other activations occur through single gateways, namely

$$S_2 = Q_2F(E_2) \quad , \quad (21b)$$
$$S_3 = Q_5F(E_5) \quad , \quad (21c)$$
$$S_4 = Q_6F(E_6) \quad . \quad (21d)$$

This set of equations is underdetermined and cannot be simply inverted because the spectrum, F(E) is being sampled at six E_i to yield only four measurements.

The importance of the single gateway materials is readily apparent from Eqs. (21b)-(21d). These can be immediately inverted to give $F(E_2)$, $F(E_5)$ and $F(E_6)$. The basic assumption necessary to obtain an approximate solution for $F(E_1)$, $F(E_3)$ and $F(E_4)$ is that the function F be continuous with continuous derivatives. In that case $F(E_3)$ and $F(E_4)$ can be obtained by interpolating between the points obtained from the single gateway isotopes. Using a polynomial fit to $F(E_2)$, $F(E_5)$ and $F(E_6)$ gives reasonable estimates for $F(E_3)$ and $F(E_4)$ as shown in Fig. 8,

Table VII

Matrix for the computation of the activations of the isotopes of Table I by the spectrum of Fig. 7.

Isotope	Activation	Energy (keV) E_1 480	E_2 761	E_3 818	E_4 1005	E_5 1078	E_6 1190
^{77}Se	S_1	Q_1		Q_3	Q_4		
^{79}Br	S_2		Q_2				
^{115}In	S_3					Q_5	
^{111}Cd	S_4						Q_6

where the results of this unfolding process are shown together with the original data for the linac spectrum.

The measurement at $F(E_1)$ is pathologically difficult and makes a good example. The extrapolation of polynomial fits is a notoriously poor procedure. Since extrapolation is needed for only one point, an alternative is to solve Eq. (21a) after substituting the values interpolated for $F(E_3)$ and $F(E_4)$. Unfortunately, $Q_1 << Q_4$ so this process requires the result be obtained as a small residue between large measurements. Nevertheless, even in this pathological case, the final value obtained for $F(E_1)$ is not too poor, as can be seen in Fig. 8.

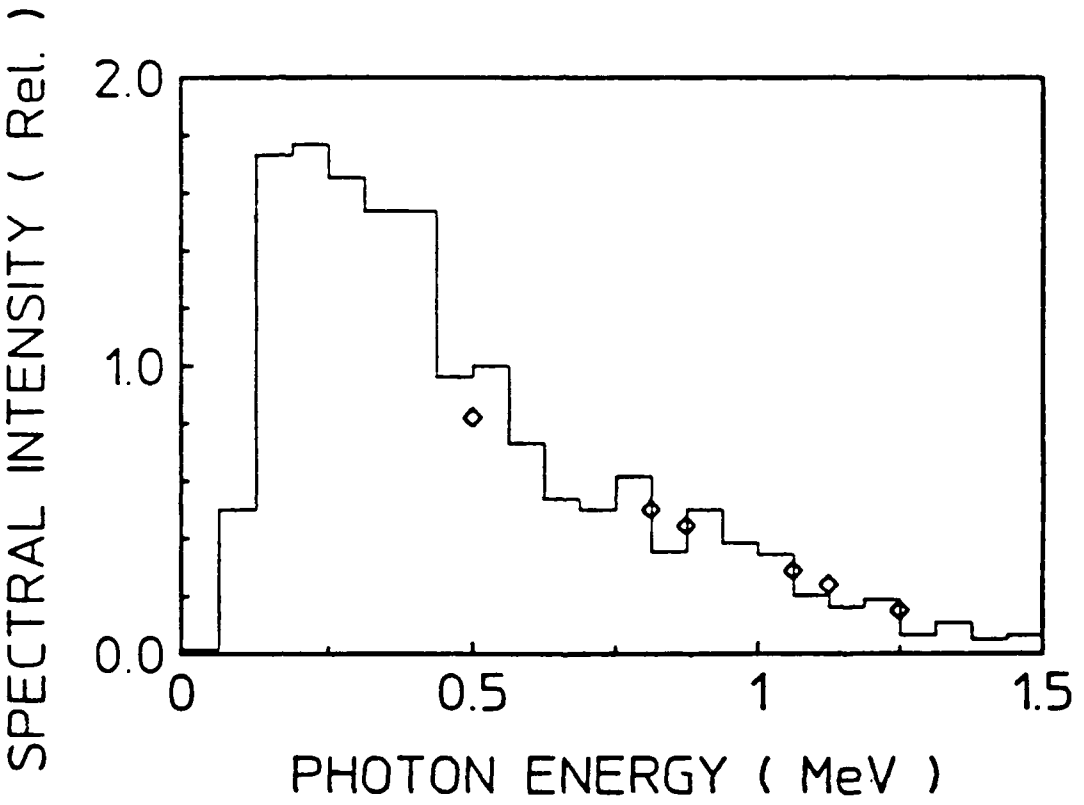

Figure 8: Plot of the hypothetical linac spectrum shown in Fig. 7, together with the values of the six measurements unfolded from simulated activations.

This example considered in Phase I is a worst case, and it is expected that the distribution of gateways in the 1.5-6.0 MeV range will be much more favorable. As discussed in previous sections, it is the selection of isotopes of Table IV that were concluded to have single gateways. Contributed by the quadrupole transitions at lower energies, the activations should be much smaller than what results from the octupole transitions at higher energies. Even if there would be only multiple gateways in the octupole region, extrapolation in this case would consist of the removal of small fitted contributions from large total activations instead of the inverse situation encountered in the example reported above. In contrast to that pathological case, the situation for the energy range 2.0 - 6.0 MeV has been shown by the Phase I work to be far more tractable. Nevertheless, even at the more difficult lower energies, the use of XAN to measure spectral intensities has already been proven in numerous examples.

The modeling of specific hypothetical cases was facilitated by the development of two software packages:

1) ENFOLD to generate synthetic activation data, and
2) UNFOLD to invert it in order to obtain the irradiating spectrum originally assumed.

Run against each other they were able to demonstrate that for likely values for the unknown nuclear parameters described above unfolded spectra could be realized with acceptable statistics when used in the targeted measurement strategy. Both programs were completed during this phase of research and documentation is reproduced in Appendix A. As can be seen there, the input spectrum $F_m(E_i)$ can be entered either as a table of values for pathological cases or may be selected with a simple keypress to correspond to a Varian CLINAC (6MeV), to AURORA, or to our

estimates for the output of a variable energy linac with end points being entered in an interactive mode.

Careful attention was given to the implementation of the correct statistical noise distribution. Since small activations are economical in terms of the amount of material required and the duration (or proximity) of the calibrating period, it was important to use Poisson distributions of counting rates. Once an activation was calculated in a particular circumstance, a random amount of noise conforming to Poisson statistics was added by the ENFOLD program to model the real uncertainty in the results of counting the decay of a single channel of activation.

In Appendix A can be seen the details of the use of these programs, together with results in illustrative cases. The unfolding of the hypothetical spectrum can be seen to be remarkably successful in the various practical cases of interest.

IV. Summary of Accomplishments

As detailed above, the achievements realized in Phase I of this research prove the clear feasibility of subsequent work. A primary norm having a single gateway for activation has been found for the 2.0 to 6.0 MeV range of Photon energies, and eleven isotopes have been identified as able to sample the spectrum at 18 points. The modeling of a preferred measurement strategy has shown that atarget composed of these materials could be manually positioned by an operator, exposed, and then transferred by the operator to a measurement station located in reasonable proximity. Counting times of only 10 minutes and exposures of either 10 minutes for a medical linac or one shot from a nuclear simulator would give adequate activation for analysis. The

modeling strategies further showed the probabilities were only 10% that a gap as large as 0.5 MeV would be left unmeasured by the selection of isotopes prescribed, and that there was far less opportunity for a pathological accident in the distribution of gateways than in the case of measurement below 1.5 MeV, already reduced to practice.

The only remaining obstacle to the actual realization of an XAN procedure for validating bremsstrahlung spectra in the 2.0 to 6.0 MeV region lies in the acquisition, installation and operation of a variable energy linac with which the gateways for sampling spectral intensities can be pinpointed.

V. References

1. C. B. Collins, F. W. Lee, D. M. Shemwell, B. D. DePaola, S. Olariu, and I. I. Popescu, J. Appl. Phys. 53, 4645 (1982).
2. Center for Quantum Electronics, Quarterly Technical Report No. GRL/8702, University of Texas at Dallas, (Oct, 1987).
3. C. B. Collins, in Center for Quantum Electronics, Annual Technical Report No. GRL/8603, University of Texas at Dallas, (Oct, 1987) p.iii.
4. C. B. Collins, Center for Quantum Electronics, Major Milestone Report, University of Texas at Dallas, (October 16, 1987) .
5. R. Mohan, C. Chui, and L. Lidiofsky, Med. Phys. 12, 592 (1985).
6. J. A. Halbleib and T. W. Sanford, Sandia Report SAND832572 (1983).
7. J. A. Anderson and C. B. Collins, Rev. Sci. Instrum. 58, 2157 (1987).

8. J. A. Anderson and C. B. Collins, Rev. Sci. Instrum. 59, 414 (1988).
9. C. B. Collins, C. D. Eberhard, J. W. Glesener, and J. A. Anderson, Phys. Rev. C. 37, 2267 (1988).
10. Above 6.0 MeV photons may dislodge neutrons which quickly produce an unbearable problem of heating.
11. C. B. Collins, J. A. Anderson, Y. Paiss, C. D. Eberhard, R. J. Peterson, and W. L. Hodge, Phys. Rev. C. 38, 1852 (1988)..
12. J. A. Anderson, M. J. Byrd, and C. B. Collins, Phys. Rev. C (pending).
13. J. A. Anderson and C. B. Collins, in Center for Quantum Electronics, Quarterly Technical Report No. GRL/8701, University of Texas at Dallas, (July, 1987) p. 18-21.
14. C. B. Collins and J. A. Anderson, in Center for Quantum Electronics, Quarterly Technical Report No. GRL/8701, University of Texas at Dallas, (July, 1987) p. 35-53.
15. Evaluated Nuclear Structure Data File (Brookhaven National Laboratory, Upton, New York, 1986).
16. J. A. Anderson, C. D. Eberhard, J. J. Carroll, M. J. Byrd, C. B. Collins, E. Scarbrough and P. P. Antich, in Center for Quantum Electronics, Quarterly Technical Report No. GRL/8801, University of Texas at Dallas, (July, 1988) p. 45.
17. B. T. Chertok and E. C. Booth, Nuc. Phys. 66, 230 (1965).
18. J. A. Anderson, C. D. Eberhard, J. J. Carroll, M. J. Byrd, C. B. Collins, E. Scarbrough and P. P. Antich, in Center for Quantum Electronics, Quarterly Technical Report No. GRL/8801, University of Texas at Dallas, (July, 1988) p. 15-42.
19 As mentioned earlier, for the single particle states the cross sections for the excitation of isomers should be limited to values of the order of 1-3 as found in Table I.
20. C. B. Collins, in Center for Quantum Electronics, Quarterly

Technical Report No. GRL/8701, University of Texas at Dallas, (July, 1987) p 1-10.

21. P. J. Brussard and P. W. M. Glaudemans, Shell Model Applications in Nuclear Spectroscopy, (North-Holland, Amsterdam 1977) p. 203.

22. C. B. Collins, S. Olariu, M. Petrascu, and I. I. Popescu, Phys. Rev. Lett. 42, 1397 (1979).

Appendix I

Review of the ENFOLD and UNFOLD programs for generating and deconvolving synthetic data.

A major project goal for Phase I was met by the development of two programs which allowed the simulation of a spectral calibration. The first, called ENFOLD, is an accurate, convenient and fast method of generating hypothetical data sets for the activation and for the observed photopeak counts resulting from the exposure of selected nuclei to typical flash and cw x-ray spectra. These sets of data formed the basis for the development and testing of the second program, UNFOLD, a deconvolution procedure capable of determining the incident x-ray spectra from the photopeaks observed in nuclear fluorescence spectra of isomeric decays in a particular set of target materials.

ENFOLD

ENFOLD was created in a Lotus 1-2-3 spreadsheet. This format was chosen for its graphing, editing and custom menu features. The program takes into account many factors in order to accurately simulate data measured with standard scintillator spectrometer techniques:

1. Nuclear - Each chosen nucleus possessing an isomeric state has its own set of nuclear parameters, such as natural abundance, half-life of the isomer, dominant decay fluorescence energies, and relative intensities of the signature photons[1]. Of primary importance for each nucleus are the integrated cross sections $(\sigma\Gamma)_i$ and energies E_i of the gateways through which

photoactivation proceeds[2]. These parameters must be manually entered by the operator.

2. Detector - The operator has an option for each of the selected nuclei to choose with which of 3 typical detectors the sample was counted in the simulation. The options are between a 3" x 3" solid NaI(Tl) detector, a 3" x 3" well NaI(Tl) detector, or a 2" x 2" solid, high purity germanium detector. The choice is made through a custom menu in the spreadsheet and provides detector efficiencies at the fluorescence energies[3].

3. Self-Absorption - Due to the finite thickness of typical samples, some self absorption of fluorescence photons occurs and a suitable correction must be made. This is calculated from the chosen detector and typical sample geometry separately by Monte-Carlo methods, and manually entered into the spreadsheet[4].

4. Decay - Correction is automatically made to take into account the decay during transport of samples to the detector, counting of the samples, and in the case of exposure to cw x-ray spectra, during the irradiation[4].

5. Spectrum - The operator may choose to simulate irradiation of the samples with a variety of typical spectra, or may enter an arbitrary spectra. Spectra included in the spreadsheet are smoothed transport code evaluations of 1.5 to 6 MeV endpoint cw linac spectra (normalized to the output of a Varian Clinac 1800 operating at 300 Hz in a 6 MeV photon mode)[5] and of 6 to 10 MeV endpoint flash spectra obtained from the DNA/AURORA nuclear simulator[6]. These choices are made

through custom menus. Once a spectrum is chosen, the program automatically calculates the hypothetical, exact activation for each target material from

$$Act = \Sigma_i (\sigma\Gamma)_i \phi(E_i) \qquad (1)$$

where $\phi(E_i)$ is the flux at the gateway energy E_i. Spectra may be plotted in several different formats through a custom menu.

6. Random deviates - Observed photopeaks always contain statistical variation due to the natural Poisson distribution of the decay events. The operator may choose to generate observed counts directly from the exact activation or to include the statistical effect by generating random Poisson deviates about the exact number of counts.[7] This is done through a custom menu.

UNFOLD

The UNFOLD program was written in MS-Fortran in order to utilize its strong debugging capability. The deconvolution of an irradiating spectrum from the activations present in target materials depends primarily on a full knowledge of the cross sections for photoactivation and their energy locations for each material. At this time, this information is not available. However, in accordance with the nuclear systematic study discussed previously it is possible to model a set of likely nuclear parameters by the following assumptions:

1. There exist a set of four isomeric nuclei, ^{87}Sr, ^{89}Y, ^{137}Ba and ^{199}Hg which are activated through single gateways located between 1.5 and 3 MeV. Within this range, the gateways were placed randomly and their

cross sections taken directly from reference 2.

2. There exist a set of seven isomeric nuclei, ^{77}Se, ^{111}Cd, ^{113}In, ^{115}In, ^{135}Ba, ^{179}Hf and ^{195}Pt which are activated through two gateways, one laying between 1.5 and 3 MeV, and the other laying between 4 and 6 MeV. Within each range the gateways were located randomly. For each material, the cross section of the upper gateway was taken to be 10 times larger than that of the lower gateway. Values for the cross sections were determined from reference 2 by employing eq. 1 and the spectrum of the device used in these experiments to irradiate the samples, the aforementioned linac operating in the 6 MeV mode.

The modeling procedure was to determine the flux at each of the single gateway locations and then to fit a curve to these points, using general least squares methods. This enabled the flux to be calculated at the positions of the lower gateways in each multiple gateway material. The contribution to the total activation for these materials from the lower gateways was then be removed and the flux at the location of the upper gateways found using eq. 1.

Three examples of the use of UNFOLD are included here to illustrate the degree to which this approach has been successful in deconvolving the irradiating spectrum. Example 1 shows the results of a 3 MeV endpoint irradiating linac spectrum. In this example none of the upper gateways of the multiple gateway materials were accessed. Example 2 shows the results of a 4.5 MeV end point linac spectrum in which some, but not all, of the upper gateways were accessed. Finally, example 3 displays the unfolding of a 6 MeV end point linac spectrum in which all gateways are accessed. In each case the extent to which the

irradiating x-ray spectrum was reproduced at the gateway locations was remarkable. The high degree of success achieved using this model is indicative of the potential of the XAN technique. The problem remains to experimentally determine the locations and cross sections for photoactivation for a wide range of nuclei, a problem which cannot be adequately addressed at this time.

FOOTNOTES

1. E. Browne & R. B. Firestone, Table of Radioactive Isotopes, Ed. by V.S. Shirley (John Wiley & Sons, New York, 1986).

2. Integrated cross sections obtained from Center for Quantum Electronics Reports #GRL/8701, 8702, 8703, 8704, 8801, 8802, 8803, and 8804, University of Texas at Dallas.

3. Detector information obtained from Center for Quantum Electronics, University of Texas at Dallas, private communication.

4. See for Example: G.F. Knoll, Radiation Detection and Measurement (John Wiley & Sons, New York, 1979).

5. R. Mohan, C. Chui & L. Lidofsky, Med. Phys. 12, 595 (1985).

6. K. G. Kerris, The Aurora Bremsstrahlung Environment, HDL-TM-81-18 Harry Diamonds Laboratories, Adelphi, Md., and private communications.

7. W.H. Press, B.P. Flannery, S.A. Teukosky & W.T. Vettering, Numerical Recipes: The Art of Scientific Programming (Cambridge University Press, New York, 1988).

EXAMPLE 1 - 3 MeV

DATA GENERATION PROGRAM - (ENFOLD) - Produces observed counts representing activations present in hypothetical samples due to a particular given input x-ray spectrum.

General Instructions

Choices of input spectrum, detector efficiencies, type of random deviates, and spectral plot (if desired) are made through menus.

Spectrum menu - Linac,Arbitrary or Aurora - Alt-S
Detector menu - NaI well or solid or HPGe well - Alt-D
Random deviates menu - Exact or Poisson - Alt-R
Spectral plot menu - Linear,Log or MeV/MeV - Alt-P

Spectrum: Linac EEnd[MeV]= 3

Detector: Isomer1: 3" x 3" NaI well
Isomer2: 3" x 3" NaI well
Isomer3: 3" x 3" NaI well
Isomer4: 3" x 3" NaI well

Rand dev: Poisson

Spectral Distribution

Energy[MeV]	Phi[1/cm^2-keV-sec]
0.063	1.47E+08
0.188	4.79E+09
0.313	1.69E+10
0.438	1.67E+10
0.563	1.64E+10
0.688	1.55E+10
0.813	1.38E+10
0.938	1.06E+10
1.063	8.69E+09
1.188	7.23E+09
1.313	6.08E+09
1.438	5.16E+09
1.563	4.41E+09
1.688	3.80E+09
1.813	3.28E+09
1.938	2.86E+09
2.063	2.49E+09
2.188	2.10E+09
2.313	1.77E+09
2.438	1.42E+09
2.563	1.09E+09
2.688	8.02E+08
2.813	5.63E+08
2.938	3.77E+08

Target Isomer Information
Single gateway nuclei

Isomer1- 87Sr		Isomer2- 89Y	
NTargets= 1.0E+20		Ntargets= 1.0E+22	
EGate[MeV]	SG[10^-29cm^2-keV]	EGate[MeV]	SG[10^-29cm^2-keV]
2.66	2008	2.79	592
0	0	0	0
0	0	0	0
0	0	0	0
0	0	0	0
0	0	0	0
ExactAct[1/sec]=	1.73E-17	ExactAct[1/sec]=	3.56E-18
T1/2[s] =	1.01E+04	T1/2[s] =	1.61E+01
IrrT[s] =	300	IrrT[s] =	300
TT[s] =	60	TT[s] =	60
CntT[s] =	300	CntT[s] =	300
DecCorr1=	2.03E-02	DecCorr1=	7.55E-02
DecCorr2=	9.90E-01	DecCorr2=	7.74E-02
DeadTCor=	1.00E+00	DeadTCor=	1.00E+00
E1[keV] =	388.4	E1[keV] =	909.15
Intens =	0.823	Intens =	0.9914
SelfAbs =	1.000	SelfAbs =	1.000
DetEff =	0.339	DetEff =	0.102
ObsCts1 =	2937	ObsCts1 =	6255
StandDev=	54	StandDev=	79
E2[keV] =	0	E2[keV] =	0
Intns =	0	Intens =	0
SelfAbs =	0.000	SelfAbs =	0.000
DetEff =	0.000	DetEff =	0.000
ObsCts2 =	0	ObsCts2 =	0
StandDev=	0	StandDev=	0

Isomer3- 137Ba NTargets= 1.0E+19		Isomer4- 199Hg Ntargets= 1.0E+19	
EGate[MeV]	SG[10^-29cm^2-keV]	EGate[MeV]	SG[10^-29cm^2-keV]
1.99	2203	2.83	3698
0	0	0	0
0	0	0	0
0	0	0	0
0	0	0	0
0	0	0	0
ExactAct[1/sec]=	6.01E-17	ExactAct[1/sec]=	1.97E-17
T1/2[s] =	1.53E+02	T1/2[s] =	2.56E+03
IrrT[s] =	300	IrrT[s] =	300
TT[s] =	60	TT[s] =	60
CntT[s] =	300	CntT[s] =	300
DecCorr1=	5.66E-01	DecCorr1=	7.69E-02
DecCorr2=	5.47E-01	DecCorr2=	9.60E-01
DeadTCor=	1.00E+00	DeadTCor=	1.00E+00
E1[keV] =	661.66	E1[keV] =	158.376
Intens =	0.901	Intens =	0.53
SelfAbs =	1.000	SelfAbs =	1.000
DetEff =	0.181	DetEff =	0.577
ObsCts1 =	9089	ObsCts1 =	1372
StandDev=	95	StandDev=	37
E2[keV] =	0	E2[keV] =	0
Intens =	0	Intens =	0
SelfAbs =	0.000	SelfAbs =	0.000
DetEff =	0.000	DetEff =	0.000
ObsCts2 =	0	ObsCts2 =	0
StandDev=	0	StandDev=	0

Target Isomer Information
Multiple gateway nuclei

Isomer1- 77Se NTargets= 1.0E+21		Isomer2- 111Cd Ntargets= 1.0E+20	
EGate[MeV]	SG[10^-29cm^2-keV]	EGate[MeV]	SG[10^-29cm^2-keV]
1.75	289	1.62	53
4.12	2891	4.26	529
0	0	0	0
0	0	0	0
0	0	0	0
0	0	0	0
ExactAct[1/sec]=	1.02E-17	ExactAct[1/sec]=	2.18E-18
T1/2[s] =	1.75E+01	T1/2[s] =	2.92E+03
IrrT[s] =	300	IrrT[s] =	300
TT[s] =	60	TT[s] =	60
CntT[s] =	300	CntT[s] =	300
DecCorr1=	9.22E-02	DecCorr1=	6.79E-02
DecCorr2=	8.39E-02	DecCorr2=	9.65E-01
DeadTCor=	1.00E+00	DeadTCor=	1.00E+00
E1[keV] =	161.92	E1[keV] =	245.384
Intens =	0.524	Intens =	0.94
SelfAbs =	1.000	SelfAbs =	1.000
DetEff =	0.572	DetEff =	0.472
ObsCts1 =	7171	ObsCts1 =	1871
StandDev=	85	StandDev=	43
E2[keV] =	0	E2[keV] =	0
Intns =	0	Intens =	0
SelfAbs =	0.000	SelfAbs =	0.000
DetEff =	0.000	DetEff =	0.000
ObsCts2 =	0	ObsCts2 =	0
StandDev=	0	StandDev=	0

Isomer3- 113In
NTargets= 5.0E+20

EGate[MeV]	SG[10^-29cm^2-keV]
1.96	80
4.51	797
0	0
0	0
0	0
0	0

ExactAct[1/sec]=	2.23E-18
T1/2[s] =	6.97E+03
IrrT[s] =	300
TT[s] =	60
CntT[s] =	300
DecCorr1=	3.40E-02
DecCorr2=	9.83E-01
DeadTCor=	1.00E+00
E1[keV] =	391.69
Intens =	0.642
SelfAbs =	1.000
DetEff =	0.337
ObsCts1 =	2486
StandDev=	50
E2[keV] =	0
Intens =	0
SelfAbs =	0.000
DetEff =	0.000
ObsCts2 =	0
StandDev=	0

Isomer4- 115In
Ntargets= 1.0E+21

EGate[MeV]	SG[10^-29cm^2-keV]
2.46	123
4.82	1228
0	0
0	0
0	0
0	0

ExactAct[1/sec]=	1.67E-18
T1/2[s] =	1.57E+04
IrrT[s] =	300
TT[s] =	60
CntT[s] =	300
DecCorr1=	1.32E-02
DecCorr2=	9.93E-01
DeadTCor=	1.00E+00
E1[keV] =	336.26
Intens =	0.458
SelfAbs =	1.000
DetEff =	0.383
ObsCts1 =	1165
StandDev=	34
E2[keV] =	0
Intens =	0
SelfAbs =	0.000
DetEff =	0.000
ObsCts2 =	0
StandDev=	0

Target Isomer Information
Multiple gateway nuclei

Isomer5- 135Ba		Isomer6- 179Hf	
NTargets= 1.0E+22		Ntargets= 1.0E+20	
EGate[MeV]	SG[10⁻²⁹cm^2-keV]	EGate[MeV]	SG[10⁻²⁹cm^2-keV]
2.95	211	2.08	494
4.21	2110	4.69	4942
0	0	0	0
0	0	0	0
0	0	0	0
0	0	0	0
ExactAct[1/sec]=	7.62E-19	ExactAct[1/sec]=	1.21E-17
T1/2[s] =	1.03E+05	T1/2[s] =	1.87E+01
IrrT[s] =	300	IrrT[s] =	300
TT[s] =	60	TT[s] =	60
CntT[s] =	300	CntT[s] =	300
DecCorr1=	2.01E-03	DecCorr1=	1.08E-01
DecCorr2=	9.99E-01	DecCorr2=	8.98E-02
DeadTCor=	1.00E+00	DeadTCor=	1.00E+00
E1[keV] =	268.27	E1[keV] =	214.31
Intens =	0.156	Intens =	0.952
SelfAbs =	1.000	SelfAbs =	1.000
DetEff =	0.448	DetEff =	0.507
ObsCts1 =	306	ObsCts1 =	1713
StandDev=	17	StandDev=	41
E2[keV] =	0	E2[keV] =	0
Intns =	0	Intens =	0
SelfAbs =	0.000	SelfAbs =	0.000
DetEff =	0.000	DetEff =	0.000
ObsCts2 =	0	ObsCts2 =	0
StandDev=	0	StandDev=	0

Isomer7- 195Pt
NTargets= 5.0E+22

EGate[MeV]	SG[10^-29cm^2-keV]
1.82	223
5.40	2232
0	0
0	0
0	0
0	0

ExactAct[1/sec]= 7.26E-18

T1/2[s] =	3.47E+05
IrrT[s] =	300
TT[s] =	60
CntT[s] =	300
DecCorr1=	5.98E-04
DecCorr2=	1.00E+00
DeadTCor=	1.00E+00
E1[keV] =	129.76
Intens =	0.02885
SelfAbs =	1.000
DetEff =	0.616
ObsCts1 =	1095
StandDev=	33
E2[keV] =	0
Intens =	0
SelfAbs =	0.000
DetEff =	0.000
ObsCts2 =	0
StandDev=	0

```
C:\NEWFORT\PROGRAMS>unfold
Enter 1 for a cw exposure:
1
Enter the end point energy [MeV] of the x-ray device:
3
Enter TIrr, TTrav and TCnt [sec] for the 87Sr sample:
300 60 300
Enter the number of target nuclei for the 87Sr sample:
1E20
Enter total observed and bkgnd counts in the 388 keV peak:
2937 0
Enter 0, 1 or 2 for a NaI solid, well, or HPGe detector:
1
Enter the self-absorption:
1
Enter TIrr, TTrav and TCnt [sec] for the 89Y sample:
300 60 300
Enter the number of target nuclei for the 89Y sample:
1E22
Enter total observed and bkgnd counts in the 909 keV peak:
6255 0
Enter 0, 1 or 2 for a NaI solid, well, or HPGe detector:
1
Enter the self-absorption:


1
Enter TIrr, TTrav and TCnt [sec] for the 137Ba sample:
300 60 300
Enter the number of target nuclei for the 137Ba sample:
1E19
Enter total observed and bkgnd counts in the 661 keV peak:
9089 0
Enter 0, 1 or 2 for a NaI solid, well, or HPGe detector:
1
Enter the self-absorption:
1
Enter TIrr, TTrav and TCnt [sec] for the 199Hg sample:
300 60 300
Enter the number of target nuclei for the 199Hg sample:
1E19
Enter total observed and bkgnd counts in the 158 keV peak:
1372 0
Enter 0, 1 or 2 for a NaI solid, well, or HPGe detector:
1
Enter the self-absorption:
1
Enter 1 to examine the fit employed in the single gateway region:

The  coefficients of the power series are:
A =          1,    A =   5.068595E+09
A =          2,    A =   2.818302E+09
A =          3,    A =  -3.089682E+09
A =          4,    A =   5.397999E+08
Chi squared =       1.512296

Enter TIrr, TTrav and TCnt [sec] for the 77Se sample:
```

```
300 60 300
Enter the number of target nuclei for the 77Se sample:
1E21
Enter total observed and bkgnd counts in the 162 keV peak:
7171 0
Enter 0, 1 or 2 for a NaI solid, well, or HPGe detector:
1
Enter the self-absorption:
1
Enter Tirr, TTrav and TCnt (sec) for the 111Cd sample:
300 60 300
Enter the number of target nuclei for the 111Cd sample:
1E20
Enter total observed and bkgnd counts in the 245 keV peak:
1871 0
Enter 0, 1 or 2 for a NaI solid, well, or HPGe detector:
1
Enter the self-absorption:
1
Enter Tirr, TTrav and TCnt (sec) for the 113In sample:
300 60 300
Enter the number of target nuclei for the 113In sample:
5E20
Enter total observed and bkgnd counts in the 392 keV peak:


2466 0
Enter 0, 1 or 2 for a NaI solid, well, or HPGe detector:
1
Enter the self-absorption:
1
Enter Tirr, TTrav and TCnt (sec) for the 115In sample:
300 60 300
Enter the number of target nuclei for the 115In sample:
1E21
Enter total observed and bkgnd counts in the 336 keV peak:
1165 0
Enter 0, 1 or 2 for a NaI solid, well, or HPGe detector:
1
Enter the self-absorption:
1
Enter Tirr, TTrav and TCnt (sec) for the 135Ba sample:
300 60 300
Enter the number of target nuclei for the 135Ba sample:
1E22
Enter total observed and bkgnd counts in the 268 keV peak:
306 0
Enter 0, 1 or 2 for a NaI solid, well, or HPGe detector:
1
Enter the self-absorption:
```

```
1
Enter TIrr, TTrav and TCnt [sec] for the 179Hf sample:
30[illegible] 60 300
Enter the number of target nuclei for the 179Hf sample:
1E20
Enter total observed and bkgnd counts in the 214 keV peak:
1711 0
Enter 0, 1 or 2 for a NaI solid, well, or HPGe detector:
1
Enter the self-absorption:
1
Enter TIrr, TTrav and TCnt [sec] for the 195Pt sample:
30[illegible] 60 300
Enter the number of target nuclei for the 195Pt sample:
5E20
Enter total observed and bkgnd counts in the 130 keV peak:
1095 0
Enter 0, 1 or 2 for a NaI solid, well, or HPGe detector:
1
Enter the self-absorption:



The values of gateway energy, flux and standard deviaton are:
        2.660000     8.701814E+08     1.605676E+07
        2.790000     5.993561E+08   7578291.000000
        1.980000     2.725342E+09     2.858663E+07
        2.830000     5.480612E+08     1.479626E+07
        1.750000     3.564990E+09     4.209868E+07
        1.620000     4.050392E+09     9.363972E+07
        1.960000     2.866556E+09     5.749233E+07
        2.460000     1.377697E+09     4.036368E+07
        2.950000     3.447520E+08     1.970816E+07
        2.080000     2.470555E+09     5.969197E+07
        1.820000     3.078998E+09     9.304698E+07

C:\NEWFORT\PROGRAMS>
C:\NEWFORT\PROGRAMS>
C:\NEWFORT\PROGRAMS>
C:\NEWFORT\PROGRAMS>
C:\NEWFORT\PROGRAMS>
C:\NEWFORT\PROGRAMS>
C:\NEWFORT\PROGRAMS>
C:\NEWFORT\PROGRAMS>
C:\NEWFORT\PROGRAMS>
C:\NEWFORT\PROGRAMS>
C:\NEWFORT\PROGRAMS>
```

Enfold spectrum
Fit generated by UNfold

EXAMPLE 2 - 4.5 MeV

DATA GENERATION PROGRAM - (ENFOLD) - Produces observed counts representing activations present in hypothetical samples due to a particular given input x-ray spectrum

General Instructions

Choices of input spectrum, detector efficiencies, type of random deviates, and spectral plot (if desired) are made through menus.

Spectrum menu - Linac,Arbitrary or Aurora - Alt-S
Detector menu - NaI well or solid or HPGe well - Alt-D
Random deviates menu - Exact or Poisson - Alt-R
Spectral plot menu - Linear,Log or MeV/MeV - Alt-P

Spectrum: Linac EEnd[MeV]= 4.5

Detector: Isomer1: 3" x 3" NaI well
Isomer2: 3" x 3" NaI well
Isomer3: 3" x 3" NaI well
Isomer4: 3" x 3" NaI well

Rand dev: Poisson

Spectral Distribution

Energy[MeV]	Phi[1/cm^2-keV-sec]
0.094	6.56E+07
0.281	2.14E+09
0.469	7.52E+09
0.656	7.45E+09
0.844	7.33E+09
1.031	6.91E+09
1.219	6.15E+09
1.406	4.72E+09
1.594	3.87E+09
1.781	3.22E+09
1.969	2.71E+09
2.156	2.30E+09
2.344	1.97E+09
2.531	1.69E+09
2.719	1.46E+09
2.906	1.27E+09
3.094	1.11E+09
3.281	9.36E+08
3.469	7.87E+08
3.656	6.34E+08
3.844	4.87E+08
4.031	3.58E+08
4.219	2.51E+08
4.406	1.68E+08

Target Isomer Information
Single gateway nuclei

Isomer1- 87Sr NTargets= 1.0E+20		Isomer2- 89Y Ntargets= 1.0E+22	
EGate[MeV]	SG[10^-29cm^2-keV]	EGate[MeV]	SG[10^-29cm^2-keV]
1.66	2008	2.79	592
0	0	0	0
0	0	0	0
0	0	0	0
0	0	0	0
0	0	0	0
ExactAct[1/sec]=	3.07E-17	ExactAct[1/sec]=	8.21E-18
T1/2[s] =	1.01E+04	T1/2[s] =	1.61E+01
IrrT[s] =	300	IrrT[s] =	300
TT[s] =	60	TT[s] =	60
CntT[s] =	300	CntT[s] =	300
DecCorr1=	2.03E-02	DecCorr1=	7.55E-02
DecCorr2=	9.90E-01	DecCorr2=	7.74E-02
DeadTCor=	1.00E+00	DeadTCor=	1.00E+00
E1[keV] =	388.4	E1[keV] =	909.15
Intens =	0.823	Intens =	0.9914
SelfAbs =	1.000	SelfAbs =	1.000
DetEff =	0.339	DetEff =	0.102
ObsCts1 =	5235	ObsCts1 =	14590
StandDev=	72	StandDev=	121
E2[keV] =	0	E2[keV] =	0
Intns =	0	Intens =	0
SelfAbs =	0.000	SelfAbs =	0.000
DetEff =	0.000	DetEff =	0.000
ObsCts2 =	0	ObsCts2 =	0
StandDev=	0	StandDev=	0

Isomer3- 137Ba
NTargets= 1.0E+19

EGate[MeV]	SG[10^-29cm^2-keV]
1.99	2203
0	0
0	0
0	0
0	0
0	0

ExactAct[1/sec]= 5.91E-17

T1/2[s] =	1.53E+02
IrrT[s] =	300
TT[s] =	60
CntT[s] =	300
DecCorr1=	5.66E-01
DecCorr2=	5.47E-01
DeadTCor=	1.00E+00
E1[keV] =	661.66
Intens =	0.901
SelfAbs =	1.000
DetEff =	0.181
ObsCts1 =	8744
StandDev=	94
E2[keV] =	0
Intens =	0
SelfAbs =	0.000
DetEff =	0.000
ObsCts2 =	0
StandDev=	0

Isomer4- 199Hg
Ntargets= 1.0E+19

EGate[MeV]	SG[10^-29cm^2-keV]
2.83	3698
0	0
0	0
0	0
0	0
0	0

ExactAct[1/sec]= 4.98E-17

T1/2[s] =	2.56E+03
IrrT[s] =	300
TT[s] =	60
CntT[s] =	300
DecCorr1=	7.69E-02
DecCorr2=	9.60E-01
DeadTCor=	1.00E+00
E1[keV] =	158.376
Intens =	0.53
SelfAbs =	1.000
DetEff =	0.577
ObsCts1 =	3447
StandDev=	59
E2[keV] =	0
Intens =	0
SelfAbs =	0.000
DetEff =	0.000
ObsCts2 =	0
StandDev=	0

Target Isomer Information
Multiple gateway nuclei

Isomer1- 77Se NTargets= 1.0E+21		Isomer2- 111Cd Ntargets= 1.0E+20	
EGate[MeV]	SG[10^-29cm^2-keV]	EGate[MeV]	SG[10^-29cm^2-keV]
1.15	289	1.62	53
4.12	2891	4.26	529
0	0	0	0
0	0	0	0
0	0	0	0
0	0	0	0
ExactAct[1/sec]=	1.84E-17	ExactAct[1/sec]=	3.22E-18
T1/2[s] =	1.75E+01	T1/2[s] =	2.92E+03
IrrT[s] =	300	IrrT[s] =	300
TT[s] =	60	TT[s] =	60
CntT[s] =	300	CntT[s] =	300
DecCorr1=	9.22E-02	DecCorr1=	6.79E-02
DecCorr2=	8.39E-02	DecCorr2=	9.65E-01
DeadTCor=	1.00E+00	DeadTCor=	1.00E+00
E1[keV] =	161.92	E1[keV] =	245.384
Intens =	0.524	Intens =	0.94
SelfAbs =	1.000	SelfAbs =	1.000
DetEff =	0.572	DetEff =	0.472
ObsCts1 =	12838	ObsCts1 =	2760
StandDev=	113	StandDev=	53
E2[keV] =	0	E2[keV] =	0
Intns =	0	Intens =	0
SelfAbs =	0.000	SelfAbs =	0.000
DetEff =	0.000	DetEff =	0.000
ObsCts2 =	0	ObsCts2 =	0
StandDev=	0	StandDev=	0

Isomer3- 113In NTargets= 5.0E+20		Isomer4- 115In Ntargets= 1.0E+21	
EGate[MeV]	SG[10^-29cm^2-keV]	EGate[MeV]	SG[10^-29cm^2-keV]
1.96	80	2.46	123
4.51	797	4.82	1228
0	0	0	0
0	0	0	0
0	0	0	0
0	0	0	0
ExactAct[1/sec]=	2.18E-18	ExactAct[1/sec]=	2.20E-18
T1/2[s] =	5.97E+03	T1/2[s] =	1.57E+04
IrrT[s] =	300	IrrT[s] =	300
TT[s] =	60	TT[s] =	60
CntT[s] =	300	CntT[s] =	300
DecCorr1=	3.40E-02	DecCorr1=	1.32E-02
DecCorr2=	9.83E-01	DecCorr2=	9.93E-01
DeadTCor=	1.00E+00	DeadTCor=	1.00E+00
E1[keV] =	391.69	E1[keV] =	336.26
Intens =	0.642	Intens =	0.458
SelfAbs =	1.000	SelfAbs =	1.000
DetEff =	0.337	DetEff =	0.383
ObsCts1 =	2404	ObsCts1 =	1474
StandDev=	49	StandDev=	38
E2[keV] =	0	E2[keV] =	0
Intens =	0	Intens =	0
SelfAbs =	0.000	SelfAbs =	0.000
DetEff =	0.000	DetEff =	0.000
ObsCts2 =	0	ObsCts2 =	0
StandDev=	0	StandDev=	0

Target Isomer Information
Multiple gateway nuclei

Isomer5- 135Ba NTargets= 1.0E+22		Isomer6- 179Hf Ntargets= 1.0E+20	
EGate[MeV]	SG[10^-29cm^2-keV]	EGate[MeV]	SG[10^-29cm^2-keV]
2.95	211	2.08	494
4.21	2110	4.69	4942
0	0	0	0
0	0	0	0
0	0	0	0
0	0	0	0
ExactAct[1/sec]=	7.99E-18	ExactAct[1/sec]=	1.21E-17
T1/2[s] =	1.03E+05	T1/2[s] =	1.87E+01
IrrT[s] =	300	IrrT[s] =	300
TT[s] =	60	TT[s] =	60
CntT[s] =	300	CntT[s] =	300
DecCorr1=	2.01E-03	DecCorr1=	1.08E-01
DecCorr2=	9.99E-01	DecCorr2=	8.98E-02
DeadTCor=	1.00E+00	DeadTCor=	1.00E+00
E1[keV] =	268.27	E1[keV] =	214.31
Intens =	0.156	Intens =	0.952
SelfAbs =	1.000	SelfAbs =	1.000
DetEff =	0.448	DetEff =	0.507
ObsCts1 =	3357	ObsCts1 =	1752
StandDev=	58	StandDev=	42
E2[keV] =	0	E2[keV] =	0
Intns =	0	Intens =	0
SelfAbs =	0.000	SelfAbs =	0.000
DetEff =	0.000	DetEff =	0.000
ObsCts2 =	0	ObsCts2 =	0
StandDev=	0	StandDev=	0

Isomer?- 195Pt
NTargets= 5.0E+22

EGate[MeV]	SG[10^-29cm^2-keV]
1.82	223
5.48	2232
0	0
0	0
0	0
0	0

ExactAct[1/sec]= 6.92E-18

T1/2[s] =	3.47E+05
IrrT[s] =	300
TT[s] =	60
CntT[s] =	300
DecCorr1=	5.98E-04
DecCorr2=	1.00E+00
DeadTCor=	1.00E+00
E1[keV] =	129.76
Intens =	0.02885
SelfAbs =	1.000
DetEff =	0.616
ObsCts1 =	1099
StandDev=	33
E2[keV] =	0
Intens =	0
SelfAbs =	0.000
DetEff =	0.000
ObsCts2 =	0
StandDev=	0

```
C:\NEWFORT\PROGRAMS>unfold
Enter 1 for a cv exposure:
1
Enter the end point energy [MeV] of the x-ray device:
4.5
Enter TIrr, TTrav and TCnt [sec] for the 87Sr sample:
300 60 300
Enter the number of target nuclei for the 87Sr sample:
1E20
Enter total observed and bkgnd counts in the 388 keV peak:
5235 0
Enter 0, 1 or 2 for a NaI solid, well, or HPGe detector:
1
Enter the self-absorption:
1
Enter TIrr, TTrav and TCnt [sec] for the 89Y sample:
300 60 300
Enter the number of target nuclei for the 89Y sample:
1E21
Enter total observed and bkgnd counts in the 909 keV peak:
14590 0
Enter 0, 1 or 2 for a NaI solid, well, or HPGe detector:
1
Enter the self-absorption:


1
Enter TIrr, TTrav and TCnt [sec] for the 137Ba sample:
300 60 300
Enter the number of target nuclei for the 137Ba sample:
1E19
Enter total observed and bkgnd counts in the 661 keV peak:
8744 0
Enter 0, 1 or 2 for a NaI solid, well, or HPGe detector:
1
Enter the self-absorption:
1
Enter TIrr, TTrav and TCnt [sec] for the 199Hg sample:
300 60 300
Enter the number of target nuclei for the 199Hg sample:
1E19
Enter total observed and bkgnd counts in the 158 keV peak:
3447 0
Enter 0, 1 or 2 for a NaI solid, well, or HPGe detector:
1
Enter the self-absorption:



1
Enter 1 to examine the fit employed in the single gateway region:
1

The  coefficients of the power series are:
n =          1,    A =    3.657987E+09
n =          2,    A =    2.115574E+09
n =          3,    A =   -2.028464E+09
n =          4,    A =    3.514063E+08
Chi squared =    4.894636E-01

Enter TIrr, TTrav and TCnt [sec] for the 77Se sample:
```

```
300 60 300
Enter the number of target nuclei for the 77Se sample:
1E21
Enter total observed and bkgnd counts in the 162 keV peak:
12838 0
Enter 0, 1 or 2 for a NaI solid, well, or HPGe detector:
1
Enter the self-absorption:
1
Enter TIrr, TTrav and TCnt [sec] for the 111Cd sample:
300 60 300
Enter the number of target nuclei for the 111Cd sample:
1E20
Enter total observed and bkgnd counts in the 245 keV peak:
2760 0
Enter 0, 1 or 2 for a NaI solid, well, or HPGe detector:
1
Enter the self-absorption:
1
Enter TIrr, TTrav and TCnt [sec] for the 113In sample:
300 60 300
Enter the number of target nuclei for the 113In sample:
5E20
Enter total observed and bkgnd counts in the 392 keV peak:


2404 0
Enter 0, 1 or 2 for a NaI solid, well, or HPGe detector:
1
Enter the self-absorption:
1
Enter TIrr, TTrav and TCnt [sec] for the 115In sample:
300 60 300
Enter the number of target nuclei for the 115In sample:
1E21
Enter total observed and bkgnd counts in the 336 keV peak:
1474 0
Enter 0, 1 or 2 for a NaI solid, well, or HPGe detector:
1
Enter the self-absorption:
1
Enter TIrr, TTrav and TCnt [sec] for the 135Ba sample:
300 60 300
Enter the number of target nuclei for the 135Ba sample:
1E22
Enter total observed and bkgnd counts in the 268 keV peak:
3357 0
Enter 0, 1 or 2 for a NaI solid, well, or HPGe detector:
1
Enter the self-absorption:
```

```
1
Enter TIrr, TTrav and TCnt [sec] for the 179Hf sample:
300 60 300
Enter the number of target nuclei for the 179Hf sample:
1E20
Enter total observed and bkgnd counts in the 214 keV peak:
1752 0
Enter 0, 1 or 2 for a NaI solid, well, or HPGe detector:
1
Enter the self-absorption:
1
Enter TIrr, TTrav and TCnt [sec] for the 195Pt sample:
300 60 300
Enter the number of target nuclei for the 195Pt sample:
5E22
Enter total observed and bkgnd counts in the 130 keV peak:
1099 0
Enter 0, 1 or 2 for a NaI solid, well, or HPGe detector:
1
Enter the self-absorption:



1

The values of gateway energy, flux and standard deviaton are:
       2.660000    1.551038E+09    2.143701E+07
       2.790000    1.398018E+09    1.157405E+07
       1.980000    2.621893E+09    2.803883E+07
       2.830000    1.376944E+09    2.345285E+07
       1.750000    3.031389E+09    0.000000E+00
       4.120000    3.349735E+08  5630891.000000
       1.620000    3.255730E+09    0.000000E+00
       4.260000    2.724333E+08    5.053730E+07
       1.960000    2.772004E+09    5.653620E+07
       2.460000    1.743112E+09    4.540216E+07
       2.950000    1.267657E+09    0.000000E+00
       4.210000    2.514475E+08  6956013.000000
       2.080000    2.526803E+09    6.036765E+07
       1.820000    3.090245E+09    9.321678E+07

C:\NEWFORT\PROGRAMS>
C:\NEWFORT\PROGRAMS>
C:\NEWFORT\PROGRAMS>
C:\NEWFORT\PROGRAMS>
C:\NEWFORT\PROGRAMS>
C:\NEWFORT\PROGRAMS>
C:\NEWFORT\PROGRAMS>
```

ENDF/B spectrum
Fit generated by UNFOLD

EXAMPLE 3 - 6 MeV

DATA GENERATION PROGRAM - (ENFOLD) - Produces observed counts representing activations present in hypothetical samples due to a particular given input x-ray spectrum

General Instructions

Choices of input spectrum, detector efficiencies, type of random deviates, and spectral plot (if desired) are made through menus.

Spectrum menu - Linac,Arbitrary or Aurora - Alt-S
Detector menu - NaI well or solid or HPGe well - Alt-D
Random deviates menu - Exact or Poisson - Alt-R
Spectral plot menu - Linear,Log or MeV/MeV - Alt-P

Spectrum: Linac EEnd[MeV]= 6

Detector: Isomer1: 3" x 3" NaI well
Isomer2: 3" x 3" NaI well
Isomer3: 3" x 3" NaI well
Isomer4: 3" x 3" NaI well

Rand dev: Poisson

Spectral Distribution

Energy[MeV]	Phi[1/cm^2-keV-sec]
0.125	3.68E+07
0.375	1.20E+09
0.625	4.22E+09
0.875	4.18E+09
1.125	4.11E+09
1.375	3.88E+09
1.625	3.45E+09
1.875	2.65E+09
2.125	2.17E+09
2.375	1.81E+09
2.625	1.52E+09
2.875	1.29E+09
3.125	1.10E+09
3.375	9.49E+08
3.625	8.21E+08
3.875	7.14E+08
4.125	6.23E+08
4.375	5.25E+08
4.625	4.42E+08
4.875	3.55E+08
5.125	2.73E+08
5.375	2.01E+08
5.625	1.41E+08
5.875	9.42E+07

Target Isomer Information
Single gateway nuclei

Isomer1- 87Sr NTargets= 1.0E+20		Isomer2- 89Y Ntargets= 1.0E+22	
EGate[MeV]	SG[10^-29cm^2-keV]	EGate[MeV]	SG[10^-29cm^2-keV]
2.66	2008	2.79	592
0	0	0	0
0	0	0	0
0	0	0	0
0	0	0	0
0	0	0	0
ExactAct[1/sec]=	2.98E-17	ExactAct[1/sec]=	8.06E-18
T1/2[s] =	1.01E+04	T1/2[s] =	1.61E+01
IrrT[s] =	300	IrrT[s] =	300
TT[s] =	60	TT[s] =	60
CntT[s] =	300	CntT[s] =	300
DecCorr1=	2.03E-02	DecCorr1=	7.55E-02
DecCorr2=	9.90E-01	DecCorr2=	7.74E-02
DeadTCor=	1.00E+00	DeadTCor=	1.00E+00
E1[keV] =	388.4	E1[keV] =	909.15
Intens =	0.823	Intens =	0.9914
SelfAbs =	1.000	SelfAbs =	1.000
DetEff =	0.339	DetEff =	0.102
ObsCts1 =	5144	ObsCts1 =	14320
StandDev=	72	StandDev=	120
E2[keV] =	0	E2[keV] =	0
Intns =	0	Intens =	0
SelfAbs =	0.000	SelfAbs =	0.000
DetEff =	0.000	DetEff =	0.000
ObsCts2 =	0	ObsCts2 =	0
StandDev=	0	StandDev=	0

Isomer3- 137Ba NTargets= 1.0E+19		Isomer4- 199Hg Ntargets= 1.0E+19	
EGate[MeV]	SG[10^-29cm^2-keV]	EGate[MeV]	SG[10^-29cm^2-keV]
1.96	2203	2.83	3698
0	0	0	0
0	0	0	0
0	0	0	0
0	0	0	0
0	0	0	0
ExactAct[1/sec]=	5.36E-17	ExactAct[1/sec]=	4.91E-17
T1/2[s] =	1.53E+02	T1/2[s] =	2.56E+03
IrrT[s] =	300	IrrT[s] =	300
TT[s] =	60	TT[s] =	60
CntT[s] =	300	CntT[s] =	300
DecCorr1=	5.66E-01	DecCorr1=	7.69E-02
DecCorr2=	5.47E-01	DecCorr2=	9.60E-01
DeadTCor=	1.00E+00	DeadTCor=	1.00E+00
E1[keV] =	661.66	E1[keV] =	158.376
Intens =	0.901	Intens =	0.53
SelfAbs =	1.000	SelfAbs =	1.000
DetEff =	0.181	DetEff =	0.577
ObsCts1 =	8027	ObsCts1 =	3390
StandDev=	90	StandDev=	58
E2[keV] =	0	E2[keV] =	0
Intens =	0	Intens =	0
SelfAbs =	0.000	SelfAbs =	0.000
DetEff =	0.000	DetEff =	0.000
ObsCts2 =	0	ObsCts2 =	0
StandDev=	0	StandDev=	0

Target Isomer Information
Multiple gateway nuclei

Isomer1- 77Se NTargets= 1.0E+21		Isomer2- 111Cd Ntargets= 1.0E+20	
EGate[MeV]	SG[10^-29cm^2-keV]	EGate[MeV]	SG[10^-29cm^2-keV]
1.75	289	1.62	53
4.12	2891	4.26	529
0	0	0	0
0	0	0	0
0	0	0	0
0	0	0	0
ExactAct[1/sec]=	2.66E-17	ExactAct[1/sec]=	4.79E-18
T1/2[s] =	1.75E+01	T1/2[s] =	2.92E+03
IrrT[s] =	300	IrrT[s] =	300
TT[s] =	60	TT[s] =	60
CntT[s] =	300	CntT[s] =	300
DecCorr1=	9.22E-02	DecCorr1=	6.79E-02
DecCorr2=	8.39E-02	DecCorr2=	9.65E-01
DeadTCor=	1.00E+00	DeadTCor=	1.00E+00
E1[keV] =	161.92	E1[keV] =	245.384
Intens =	0.524	Intens =	0.94
SelfAbs =	1.000	SelfAbs =	1.000
DetEff =	0.572	DetEff =	0.472
ObsCts1 =	18502	ObsCts1 =	4097
StandDev=	136	StandDev=	64
E2[keV] =	0	E2[keV] =	0
Intns =	0	Intens =	0
SelfAbs =	0.000	SelfAbs =	0.000
DetEff =	0.000	DetEff =	0.000
ObsCts2 =	0	ObsCts2 =	0
StandDev=	0	StandDev=	0

Isomer3- 113In
NTargets= 5.0E+20

EGate[MeV]	SG[10^-29cm^2-keV]
1.96	80
4.51	797
0	0
0	0
0	0
0	0

ExactAct[1/sec]=	5.81E-18
T1/2[s] =	5.97E+03
IrrT[s] =	300
TT[s] =	60
CntT[s] =	300
DecCorr1=	3.40E-02
DecCorr2=	9.83E-01
DeadTCor=	1.00E+00
E1[keV] =	391.69
Intens =	0.642
SelfAbs =	1.000
DetEff =	0.337
ObsCts1 =	6314
StandDev=	79
E2[keV] =	0
Intens =	0
SelfAbs =	0.000
DetEff =	0.000
ObsCts2 =	0
StandDev=	0

Isomer4- 115In
Ntargets= 1.0E+21

EGate[MeV]	SG[10^-29cm^2-keV]
2.46	123
4.82	1228
0	0
0	0
0	0
0	0

ExactAct[1/sec]=	6.69E-18
T1/2[s] =	1.57E+04
IrrT[s] =	300
TT[s] =	60
CntT[s] =	300
DecCorr1=	1.32E-02
DecCorr2=	9.93E-01
DeadTCor=	1.00E+00
E1[keV] =	336.26
Intens =	0.458
SelfAbs =	1.000
DetEff =	0.383
ObsCts1 =	4726
StandDev=	69
E2[keV] =	0
Intens =	0
SelfAbs =	0.000
DetEff =	0.000
ObsCts2 =	0
StandDev=	0

Target Isomer Information
Multiple gateway nuclei

Isomer5- 135Ba NTargets= 1.0E+22		Isomer6- 179Hf Ntargets= 1.0E+20	
EGate[MeV]	SG[10^-29cm^2-keV]	EGate[MeV]	SG[10^-29cm^2-keV]
2.95	211	2.08	494
4.21	2110	4.69	4942
0	0	0	0
0	0	0	0
0	0	0	0
0	0	0	0
ExactAct[1/sec]=	1.52E-17	ExactAct[1/sec]=	3.18E-17
T1/2[s] =	1.03E+05	T1/2[s] =	1.87E+01
IrrT[s] =	300	IrrT[s] =	300
TT[s] =	60	TT[s] =	60
CntT[s] =	300	CntT[s] =	300
DecCorr1=	2.01E-03	DecCorr1=	1.08E-01
DecCorr2=	9.99E-01	DecCorr2=	8.98E-02
DeadTCor=	1.00E+00	DeadTCor=	1.00E+00
E1[keV] =	268.27	E1[keV] =	214.31
Intens =	0.156	Intens =	0.952
SelfAbs =	1.000	SelfAbs =	1.000
DetEff =	0.448	DetEff =	0.507
ObsCts1 =	6371	ObsCts1 =	4474
StandDev=	80	StandDev=	67
E2[keV] =	0	E2[keV] =	0
Intns =	0	Intens =	0
SelfAbs =	0.000	SelfAbs =	0.000
DetEff =	0.000	DetEff =	0.000
ObsCts2 =	0	ObsCts2 =	0
StandDev=	0	StandDev=	0

Isomer7- 195Pt
NTargets= 5.0E+22

EGate[MeV]	SG[10^-29cm^2-keV]
1.82	223
5.48	2232
0	0
0	0
0	0
0	0

ExactAct[1/sec]= 1.01E-17

T1/2[s] = 3.47E+05
IrrT[s] = 300
TT[s] = 60
CntT[s] = 300
DecCorr1= 5.98E-04
DecCorr2= 1.00E+00
DeadTCor= 1.00E+00

E1[keV] = 129.76
Intens = 0.02885
SelfAbs = 1.000
DetEff = 0.616

ObsCts1 = 1652
StandDev= 41

E2[keV] = 0
Intens = 0
SelfAbs = 0.000
DetEff = 0.000

ObsCts1 = 0
StandDev= 0

```
C:\NEWPORT\PROGRAMS>unfold
Enter 1 for a cw exposure:
1
Enter the end point energy [MeV] of the x-ray device:
6
Enter TIrr, TTrav and TCnt [sec] for the 87Sr sample:
300 60 300
Enter the number of target nuclei for the 87Sr sample:
1E20
Enter total observed and bkgnd counts in the 388 keV peak:
5144 0
Enter 0, 1 or 2 for a NaI solid, well, or HPGe detector:
1
Enter the self-absorption:
1
Enter TIrr, TTrav and TCnt [sec] for the 89Y sample:
300 60 300
Enter the number of target nuclei for the 89Y sample:
1E22
Enter total observed and bkgnd counts in the 909 keV peak:
14320 0
Enter 0, 1 or 2 for a NaI solid, well, or HPGe detector:
1
Enter the self-absorption:


1
Enter TIrr, TTrav and TCnt [sec] for the 137Ba sample:
300 60 300
Enter the number of target nuclei for the 137Ba sample:
1E19
Enter total observed and bkgnd counts in the 661 keV peak:
8027 0
Enter 0, 1 or 2 for a NaI solid, well, or HPGe detector:
1
Enter the self-absorption:
1
Enter TIrr, TTrav and TCnt [sec] for the 199Hg sample:
300 60 300
Enter the number of target nuclei for the 199Hg sample:
1E19
Enter total observed and bkgnd counts in the 158 keV peak:
3390 0
Enter 0, 1 or 2 for a NaI solid, well, or HPGe detector:
1
Enter the self-absorption:
1
Enter 1 to examine the fit employed in the single gateway region:

1

The  coefficients of the power series are:
n =          1,    A =   2.942580E+09
n =          2,    A =   1.758786E+09
n =          3,    A =  -1.497582E+09
n =          4,    A =   2.387671E+08
Chi squared =   8.092223E-01

Enter TIrr, TTrav and TCnt [sec] for the 77Se sample:
```

```
300 60 300
Enter the number of target nuclei for the 77Se sample:
1E21
Enter total observed and bkgnd counts in the 162 keV peak:
18502 0
Enter 0, 1 or 2 for a NaI solid, well, or HPGe detector:
1
Enter the self-absorption:
1
Enter TIrr, TTrav and TCnt [sec] for the 111Cd sample:
300 60 300
Enter the number of target nuclei for the 111Cd sample:
1E20
Enter total observed and bkgnd counts in the 245 keV peak:
4097 0
Enter 0, 1 or 2 for a NaI solid, well, or HPGe detector:
1
Enter the self-absorption:
1
Enter TIrr, TTrav and TCnt [sec] for the 113In sample:
300 60 300
Enter the number of target nuclei for the 113In sample:
5E20
Enter total observed and bkgnd counts in the 392 keV peak:


6314 0
Enter 0, 1 or 2 for a NaI solid, well, or HPGe detector:
1
Enter the self-absorption:
1
Enter TIrr, TTrav and TCnt [sec] for the 115In sample:
300 60 300
Enter the number of target nuclei for the 115In sample:
1E21
Enter total observed and bkgnd counts in the 336 keV peak:
4726 0
Enter 0, 1 or 2 for a NaI solid, well, or HPGe detector:
1
Enter the self-absorption:
1
Enter TIrr, TTrav and TCnt [sec] for the 135Ba sample:
300 60 300
Enter the number of target nuclei for the 135Ba sample:
1E22
Enter total observed and bkgnd counts in the 268 keV peak:
6371 0
Enter 0, 1 or 2 for a NaI solid, well, or HPGe detector:
1
Enter the self-absorption:
```

```
1
Enter TIrr, TTrav and TCnt [sec] for the 179Hf sample:
300 60 300
Enter the number of target nuclei for the 179Hf sample:
1E20
Enter total observed and bkgnd counts in the 214 keV peak:
4474 0
Enter 0, 1 or 2 for a NaI solid, well, or HPGe detector:
1
Enter the self-absorption:
1
Enter TIrr, TTrav and TCnt [sec] for the 195Pt sample:
300 60 300
Enter the number of target nuclei for the 195Pt sample:
5E22
Enter total observed and bkgnd counts in the 130 keV peak:
1651 0
Enter 0, 1 or 2 for a NaI solid, well, or HPGe detector:
1
Enter the self-absorption:



1

The values of gateway energy, flux and standard deviaton are:
       2.660000    1.524077E+09    2.124987E+07
       2.790000    1.372147E+09    1.146645E+07
       1.980000    2.406901E+09    2.686467E+07
       2.830000    1.354175E+09    2.325813E+07
       1.750000    2.713751E+09    0.000000E+00
       4.120000    6.482090E+08  6759861.000000
       1.620000    2.876682E+09    0.000000E+00
       4.260000    6.003942E+08    4.566513E+07
       1.960000    2.434493E+09    0.000000E+00
       4.510000    4.864294E+08    1.529281E+07
       2.460000    1.760933E+09    0.000000E+00
       4.820000    3.834140E+08    1.775166E+07
       2.950000    1.228004E+09    0.000000E+00
       4.210000    5.949821E+08  9289119.000000
       2.080000    2.270358E+09    0.000000E+00
       4.690000    4.180527E+08    1.031957E+07
       1.820000    2.622402E+09    0.000000E+00
       5.480000    2.020995E+08    1.907023E+07

C:\NEWFORT\PROGRAMS>
C:\NEWFORT\PROGRAMS>
C:\NEWFORT\PROGRAMS>
```

Energy [MeV]
□ ENFOLD spectrum
× Fit generated by UNFOLD